https://doi.org/10.5194/egusphere-2023-3083
Preprint. Discussion started: 23 February 2024

Emerging extreme Saharan-dust events expand northward over the Atlantic and Europe prompting record-breaking PM_{10} and $PM_{2.5}$ episodes

Sergio Rodríguez[1,*], Jessica López-Darias[1]

[1]Consejo Superior de Investigaciones Científicas, IPNA CSIC, Tenerife, Canary Islands, Spain.

Correspondence to: Sergio Rodríguez (sergio.rodriguez@csic.es)

Abstract. Unprecedented extreme Saharan-dust (duxt) events have recently expanded northward, from subtropical NW Africa to the NE Atlantic and SW Europe, affecting the Canary Islands and mainland Spain. These six historic duxt episodes occurred 3-5 February 2020, 22-29 February 2020, 15-21 February 2021, 14-17 January 2022, 29 January - 1 February 2022 and 14–20 March 2022. We analysed data of 330 Governmental Air Quality Monitoring Stations (AQMSs) of Spain, where PM_{10} and $PM_{2.5}$ are measured with European EN-standards, and found that during duxt events PM_{10} concentrations are underestimated due to technical limitations of some PM_{10} monitors to properly measure extremely high concentrations. We assessed the consistency of PM_{10} and $PM_{2.5}$ data and reconstructed 1414 PM_{10} (1h average) data of 48 AQMSs by using our novel *duxt-r* method. During duxt events, 1-hour average PM_{10} and $PM_{2.5}$ concentrations were within the range 1000-6000 $\mu g/m^3$ and 400-1200 $\mu g/m^3$, respectively. The meteorological and dust modelling-reanalyses show that the intense winds leading to massive dust plumes occurred within meteorological dipoles formed by a blocking anticyclone over western Europe and a cut-off low located at the southwest, near the Canary Islands, Cape Verde or into the Sahara. These cyclones reached this region by two main paths: deviated southward from the Atlantic mid-latitudes westerly circulation by the blocking anticyclone over western Europe or deviated northward from the tropical belt. The 22-29 February 2020 event led to (24h average) PM_{10} and $PM_{2.5}$ within the range 600-1840 $\mu g/m^3$ and 200-404 $\mu g/m^3$, being the most intense dust episodes ever recorded in the Canary Islands. The 14–20 March 2022 event led to (24h average) PM_{10} and $PM_{2.5}$ values within the range 500-3070 $\mu g/m^3$ and 100-690 $\mu g/m^3$ in south-eastern, 200-1000 $\mu g/m^3$ and 60-260 $\mu g/m^3$ in central and 150-500 $\mu g/m^3$ and 75-130 $\mu g/m^3$ in northern regions of mainland Spain and to 150-430 $\mu g/m^3$ and 30-80 $\mu g/m^3$ in the Canary Islands, respectively, being the most intense dust episode ever recorded in mainland Spain. The analysis of the 2000-2022 PM_{10} and $PM_{2.5}$ time series shows that these six duxt events have no precedent in Spain. All duxt events occurred during northern-hemisphere meteorological anomalies characterised by shifted to higher latitudes subtropical anticyclones, anomalous low pressures expanding beyond the tropical belt and a mid-latitudes amplified Rossby-waves undulation; these overall features resemble the anomalies of the atmospheric circulation linked to the anthropogenic global warming.

https://doi.org/10.5194/egusphere-2023-3083
Preprint. Discussion started: 23 February 2024

1 Introduction

Airborne dust aerosol particles are a key component of the Earth System influencing on climate (Kok et al., 2023), ecosystems (Yu et al., 2015), fisheries (Rodríguez et al., 2023) and human health (Domínguez-Rodríguez et al., 2021; Tong et al., 2023). Mayor dust sources are located in North Africa, the Middle East and inner Asia (Prospero et al., 2002), accounting for 75% of global emissions; secondary sources are located in northern and southern America, southern Africa, Australia and at high latitudes(Kok et al., 2023). Because these sources are located in arid regions they have usually been considered as "natural dust-sources" (e.g. the bed of naturally dried ancient lakes (Ginoux et al., 2012; Prospero et al., 2002)); however a growing body of evidences is showing that human actions such as the soil disruption by traditional grazing and agriculture (Katra, 2020; Mulitza et al., 2010; Vukovic et al., 2021), mining (Rodríguez et al., 2011; Zafra-Pérez et al., 2023), drying of water courses and lakes (Ginoux et al., 2012; Govarchin-Ghale et al., 2021), the expansion of intensive agriculture (Lambert et al., 2020) and wildfires (Yu and Ginoux, 2022) contribute to increase dust emissions.

Dust storms cause huge socio-economic impacts linked to loos of visibility, road traffic disruption and accidents, deviation of air travel or closure of maritime and air navigation space, cardiovascular and respiratory diseases, loose of soil and a decrease in solar energy production (Cañadillas-Ramallo et al., 2022; Domínguez-Rodríguez et al., 2021; Middleton et al., 2021; Miri and Middleton, 2022; Pi et al., 2020). For this reason, a set of operational "dust services" are available to forecast and monitor dust activity by modelling and satellite observations (Mona et al., 2023). In-situ concentrations of PM_{10} and $PM_{2.5}$ (respirable particulate matter -PM- smaller than 10 and 2.5 microns, respectively) regularly measured in air quality monitoring networks are commonly used to assess dust impacts and to validate dust models (Mona et al., 2023). In southern Europe, Saharan dust events tend to increase PM_{10} concentrations up to typical values within the range 40-90 $\mu g/m^3$ (24h average values), being dust events with (24h average) PM_{10} >100 $\mu g/m^3$ unusual (Millán-Martínez et al., 2021; Pey et al., 2013).

Understanding how climate change is affecting dust emissions is a challenge as these emissions are also affected by the natural atmospheric variability (as traced by ENSO, NAO, AMO and other climatic indexes(Evan et al., 2016)), as well as by the changes in atmospheric circulation and soil properties (e.g. humidity and biological crust (Rodriguez-Caballero et al., 2022)) as the atmosphere warms due to the increasing concentrations of greenhouse gases.

Current climate models are unable to reproduce the historical increase in atmospheric dust loads observed in paleorecords (Kutuzov et al., 2019; Preunkert et al., 2019). Based on models constraining dust emissions, it has been estimated that the global dust mass load in the modern climate is ≈ 56% higher than in pre-industrial times (Kok et al., 2023), with a maximum dust load in the mid-1980s and a subsequent decrease attributed to a decrease in North African and Asian dust emissions linked to a slowdown of the atmospheric circulation interconnected to global warming (Evan et al., 2016; Liu et al., 2020; Ridley et al., 2014). In this scenario of decreasing dust trend in North Africa and Asia, a series of unexpected extreme dust-events have recently occurred.

https://doi.org/10.5194/egusphere-2023-3083
Preprint. Discussion started: 23 February 2024

In March 2018 a "*record-breaking Saharan dust plume*" crossed the Eastern Mediterranean (Kaskaoutis et al., 2019), leading to PM_{10} values of up to (1h-average) 6000 μg/m^3 (Solomos et al., 2018), a three-fold increase in hospital admissions (Lorentzou et al., 2019; Monteiro et al., 2022) and an accelerated snow melting in the Caucasus (Dumont et al., 2020). In June 2020 the so-called "*Godzilla record-breaking trans-Atlantic African dust plume*" (Bi et al., 2023; Francis et al., 2020, 2022; Pu and Jin, 2021) led to (24h average) values PM_{10} = 453 μg/m^3 in the Caribbean and PM_{10} and $PM_{2.5}$ values = 135 and 74 μg/m^3 in southern United States (Yu et al., 2021), respectively. In March 2021, "*record-breaking dust events*" in China (Gui et al., 2022) led to (1h-average) PM_{10} and $PM_{2.5}$ values of up to 7525 μg/m^3 and 685 μg/m^3, respectively (Filonchyk and Peterson, 2022; Zhang et al., 2023). In November 2021, an "*extreme dust storm*" in Uzbekistan led to (1h average) PM_{10} and $PM_{2.5}$ concentrations of up to 4575 μg/m^3 and 705 μg/m^3 (Nishonov et al., 2023; Xi et al., 2023) .

In this study we present a set of unprecedented extreme dust-events that have recently (2020-2022) expanded northward, from North Africa, to the Atlantic and Europe prompting record-breaking PM_{10} and $PM_{2.5}$ episodes in Spain. The increase in dust activity in this region has recently been studied based on aerosol optical depth - satellite measurements (Cuevas et al., 2023). We also focused on the analysis of the consistency of PM_{10} and $PM_{2.5}$ data in the Governmental Air Quality Monitoring Networks during the extreme dust events due to the importance of having suitable data in the public databases used for health effects studies, model validation and constrains etc… (Mona et al., 2023). Understanding these emerging extreme dust events is crucial for this region, since climate projections forecast the expansion of the North African drylands toward the northwest, increasing the risk of desertification of Spain and Portugal as the subtropical anticyclone expands in a warming climate (Cresswell-Clay et al., 2022; Guiot and Cramer, 2016).

2 Methodology

2.1 Data of PM_{10} and $PM_{2.5}$

We analysed the 2000-2022 data of PM_{10} and $PM_{2.5}$ recorded in 330 stations of the Governmental Air Quality Monitoring Network of Spain distributed across the 12 Autonomous Regions of Spain and the Autonomous Spanish city of Ceuta. These stations are integrated in the European Air Quality Monitoring Network, which is the largest European infrastructure for PM_{10} and $PM_{2.5}$ monitoring following standardized methods for measurements, quality assurance (QA) and quality control (QC) (EN-16450:2017 and EN-12341:2015). In these stations, high temporal (10 to 60 minutes) resolution PM_{10} and $PM_{2.5}$ data are obtained using automatic monitors based on different principle of measurement, such as beta attenuation, tapered element oscillating microbalance and optical particle sizers (Rodríguez et al., 2012), with technical specifications accomplishing the EN-16450:2017 standard. Data of 24h average PM_{10} and $PM_{2.5}$ are also obtained with the gravimetric reference method (EN-12341:2015), used for QA/QC assessments and for converting the PM_{10} and $PM_{2.5}$ data obtained with the automatic devices to gravimetric equivalent data by using the European reference protocols (EN-16450:2017). The PM_{10} and $PM_{2.5}$ data that we

https://doi.org/10.5194/egusphere-2023-3083
Preprint. Discussion started: 23 February 2024

used were provided by the Ministry of Ecological Transition and Demographic Challenge of Spain and by the air quality departments of the Autonomous Regions.

2.2 Complementary modelling and satellite data

We also used data of the National Center for Environmental Prediction/National Center for Atmospheric Research (NCEP/NCAR) meteorological reanalysis (Kalnay et al., 1996), of the Modern-Era Retrospective analysis for Research and Applications, Version 2 (MERRA-2) model dust reanalysis (Gelaro et al., 2017) and of satellite Visible Infrared Imaging Radiometer Suite (VIIRS) sensor abord the Suomi polar satellite.

3 Results and discussion

The set of extreme dust events, to which we will refer with the acronyms *duxt* or *dx* episodes, occurred on 3-5 February 2020 (dx-01), 22-29 February 2020 (dx-02), 15-21 February 2021 (dx-03), 14-17 January 2022 (dx-04), 29 January - 1 February 2022 (dx-05), and 14–20 March 2022 (dx-06). These duxt events were characterised by dark and reddish “apocalyptic” skies (Fig.1A-1C). National Spanish and international media (Fig.1), the European Copernicus (Fig.1D) and NASA - Earth Observatory (Fig.1E) platforms reported on these historic events and their impacts on socio economical activities. During the impact of the duxt-02 event in the Canary Islands, record-breaking temperatures occurred, wildfires were favoured by the windy and dry conditions, solar production energy dropped by a 70%, maritime and air navigation space was closed, and thousands of flights were cancelled with huge economic implications due to the transfer of tourists between the Canary Islands and Europe (Fig.1)(Cuevas et al., 2021).

https://doi.org/10.5194/egusphere-2023-3083
Preprint. Discussion started: 23 February 2024

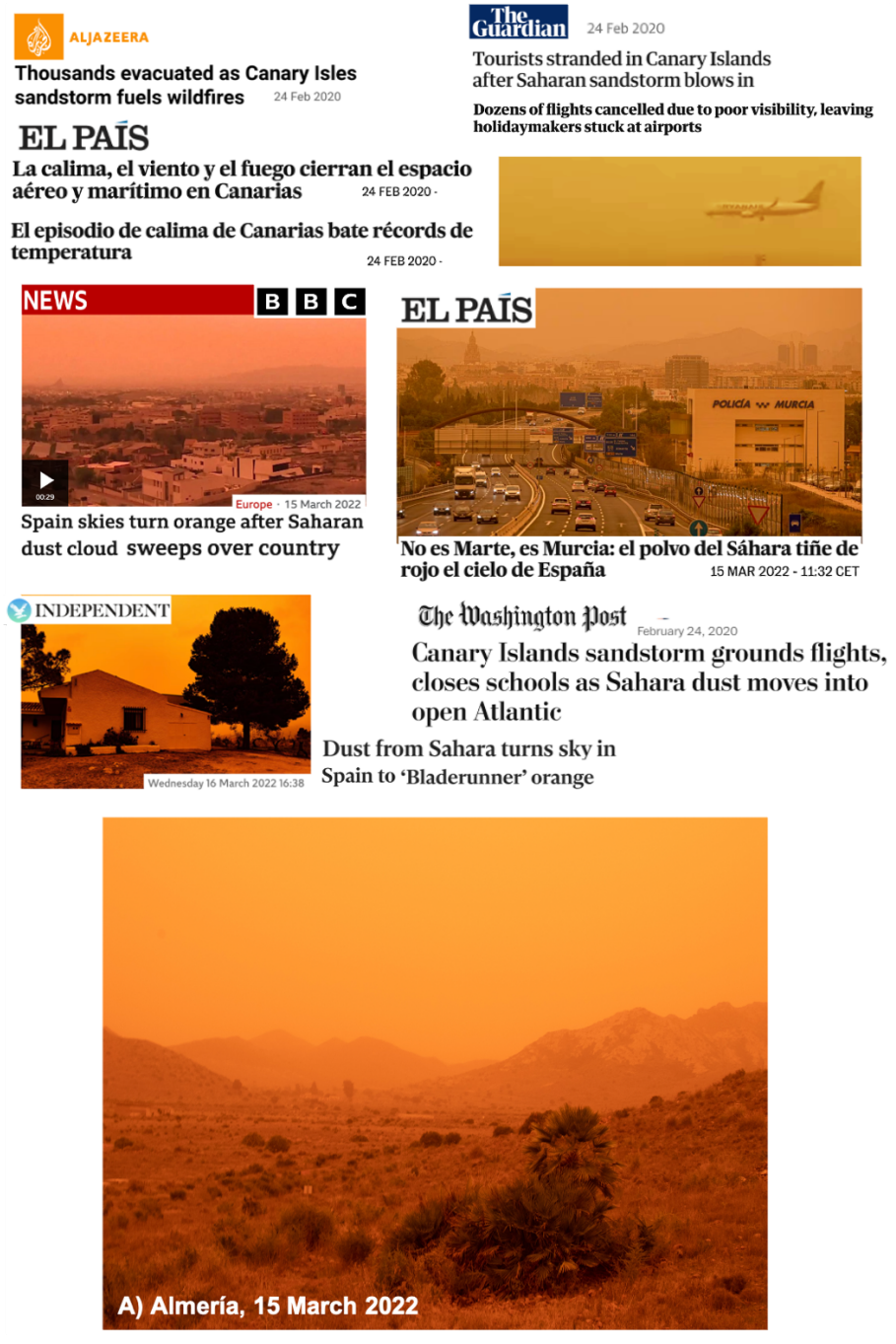

Figure 1. News on the extreme dust events impacting mainland Spain and the Canary Islands published in international and Spanish national media. Picture of the Cabo de Gata in south-eastern mainland Spain (Almería province) the 15 of March 2022 (dx-06) (taken and provided by Eva de Mas Castroverde).

5

https://doi.org/10.5194/egusphere-2023-3083
Preprint. Discussion started: 23 February 2024

Figure 1 (continue). Pictures of Tenerife (Canary Islands) the 23 of February 2020 (dx-02) and 30 of January 2022 (dx-05) (taken by the authors). Composite of the websites of Copernicus (https://atmosphere.copernicus.eu/historical-saharan-dust-episode-western-europe-cams-predictions-accurate) and Earth Observatory (https://earthobservatory.nasa.gov/images/149588/an-atmospheric-river-of-dust) reporting on the historic dust event the 15th of March 2022.

https://doi.org/10.5194/egusphere-2023-3083
Preprint. Discussion started: 23 February 2024

3.1 Assessment and reconstruction of PMx data during the duxt events

We analysed the data of PM_{10} and $PM_{2.5}$ (PM_x) of 330 Air Quality Monitoring Stations (AQMS) of the 12 Autonomous Regions of Spain and the Spanish Autonomous City of Ceuta. We found that during the duxt events, the ½ hour and 1 hour resolution data of PM_{10} increased up to reach a rather constant 'saturation' value, that in most of cases was somewhat lower than 1000 $\mu g/m^3$ (in many cases between 900 and 1000 $\mu g/m^3$), no values above this threshold appear in the data records. In these cases, PM_{10} concentrations remained constant during the period of extremely high dust concentrations (typically 5 to 30 hours), a behaviour that was not observed in $PM_{2.5}$, which exhibited a regular variability (with values < 1000 $\mu g/m^3$) and even increases in the periods when PM_{10} remained (un-consistently) constant. This behaviour can be observed in the time series of PM_{10} (Fig.2A1-A3) and $PM_{2.5}$ (Fig.2B1-B3) linked to the dx-01, dx-02, dx-04, dx-05 and dx-06 events (dx-03 is not included in Fig.2 for the sake of brevity). This saturation threshold close to ≈1000 $\mu g/m^3$ is the upper operation limit of some PM_{10} monitors and is also the top value of the validation data flag in some data recording commercial software used in many governmental air quality monitoring networks, which assume that PM_{10} concentrations above this threshold may suffer underestimation due to the high load of particles (e.g. accumulated in the filter-tape of the beta instrument or particle coincidence problems in the optical particle sizers leading to a loose of sensitivity) and consequently do not record values above this threshold. In some AQMSs the saturation threshold was found at 500 $\mu g/m^3$ and even at 200 $\mu g/m^3$. In fact, the EN-16450:2017 / 12341 /14907 certifications for PM_{10} and/or $PM_{2.5}$ monitors available in the European market are obtained for specific ranges, whose most frequent upper limit is 1000 $\mu g/m^3$ for many monitors (e.g. Met One™ BAM-1020, Comde Derenda™ APM 2 and Thermo Fisher Scientific™ 5014i, 5030i SHARP, TEOM 1405-F and 1405-DF), although is as low as 200 $\mu g/m^3$ for some equipment's (FAI™ Swam 5a) and as high as 10000 $\mu g/m^3$ for other devices (e.g. PALAS™ Fidas 200 and 200E) according to the certifications agencies (e.g. TÜV, see https://www.qal1.de/). In all these cases of PM_{10} data affected by saturation, we reconstructed the PM_{10} concentrations with the method described in Fig. 3, which we have called *duxt-r* "PM_x evaluation and reconstruction method based on ratios during extreme dust events".

In this duxt-r method: 1) we first identified the invalid 1 hour (or ½ hour or 10 minutes time resolution) PM_{10} data affected by saturation and the associated invalid $PM_{2.5}/PM_{10}$ ratios, highlighted with red circles in the example of the dx-04 event shown in Fig. 3A and 3B, 2) then, the $PM_{2.5}/PM_{10}$ ratio during the PM_{10} saturation period was estimated by interpolation between the last valid $PM_{2.5}/PM_{10}$ data before saturation and the first valid $PM_{2.5}/PM_{10}$ after saturation [$R_{2.5/10}(i)$], highlighted with green points in Fig. 3B, 3) finally, the 1 hour (or ½ hour or 10 minutes) resolution PM_{10} concentrations were determined with equation-01.

$$PM_{10} = \frac{PM_{2.5}}{R_{2.5/10}(i)} \quad (1)$$

https://doi.org/10.5194/egusphere-2023-3083
Preprint. Discussion started: 23 February 2024

We found that the $PM_{2.5}/PM_{10}$ ratio during the duxt events were within the range 0.16 to 0.22 in most of AQMSs, a value lower than that observed during regular dust events (typically ≈0.3) and much lower than that observed in environments affected by secondary particle formation and by vehicle exhaust and other combustion emissions (typically within 0.6-0.9)(Rodríguez and López-Darias, 2021).

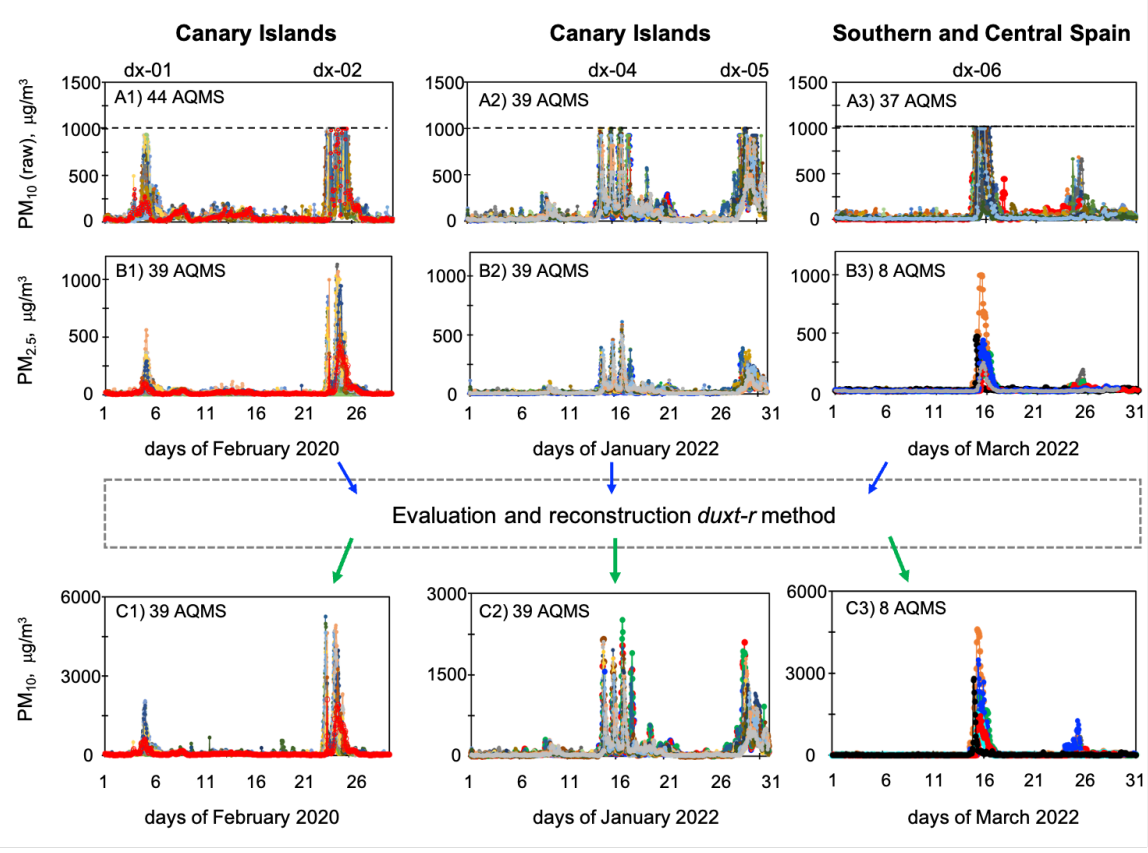

Figure. 2. Time series of 1h average PM_{10} (raw) (A1-A3) and $PM_{2.5}$ (B1-B) and evaluated and reconstructed PM_{10} data (C1-C3) during February 2020, January 2022 and March 2022, indicating the duxt events. The number of AQMSs included in each plot is shown. PM_{10} (raw) means original raw (non-reconstructed) data (A1-A3). Data of $PM_{2.5}$ are also raw (B1-B3). PM_{10} data of plots C1-C3 combines measured valid and reconstructed data.

https://doi.org/10.5194/egusphere-2023-3083
Preprint. Discussion started: 23 February 2024

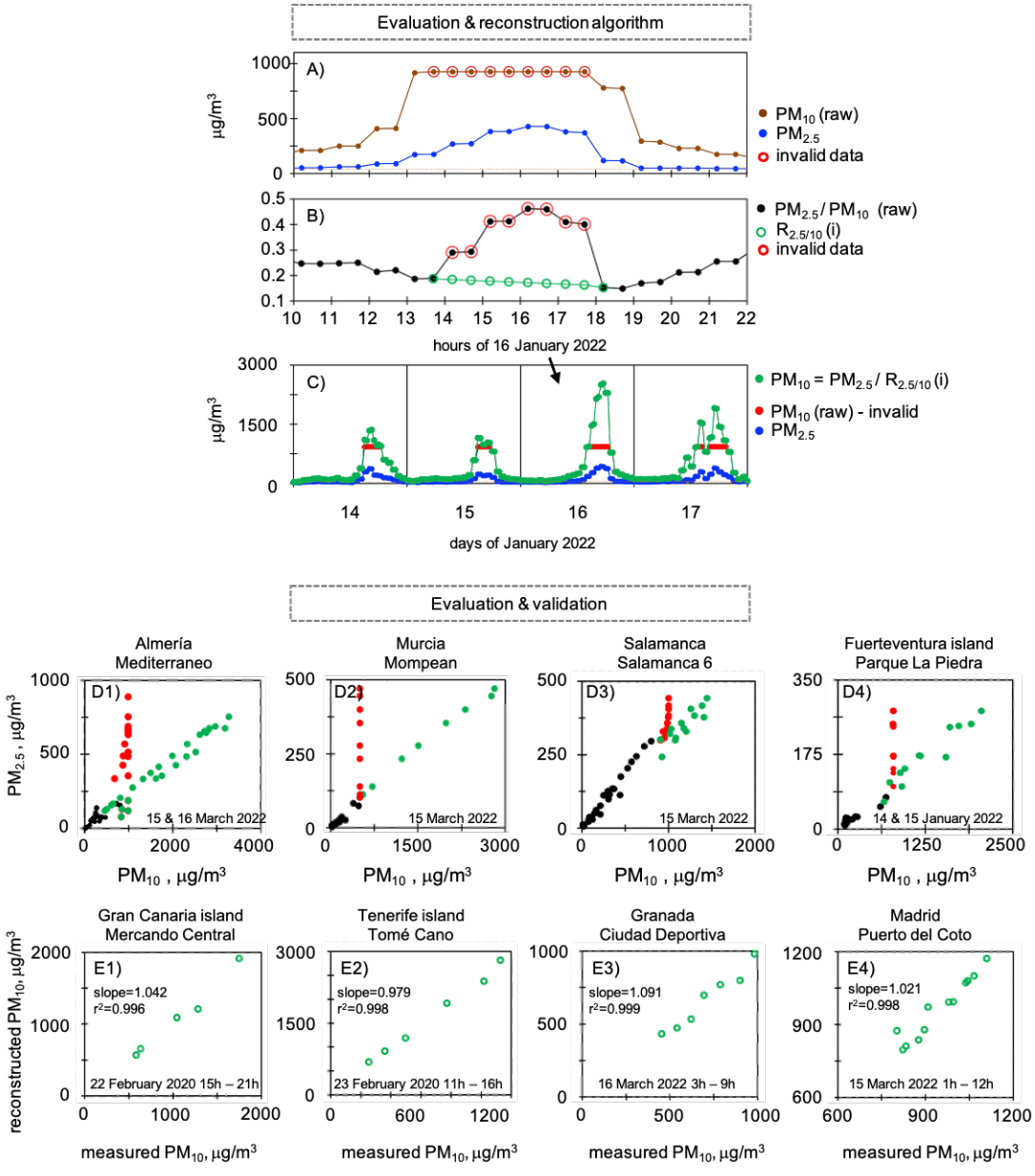

Figure 3. Evaluation, reconstruction and validation of data with the duxt-r method. Plots (A-C) shows data of El Charco site (Fuerteventura) during dx-04 event (14-17 January 2022): (A) data of PM_{10} (raw, i.e. including saturated values) and $PM_{2.5}$, (B) the measured $PM_{2.5}/PM_{10}$ (raw) ratio and the interpolated $PM_{2.5}/PM_{10}$ ratio [$R_{2.5/10}(i)$], and (C) $PM_{2.5}$, PM_{10} (raw) and PM_{10} reconstructed data. Invalid data due to PM_{10} underestimation are highlighted with red circle (A and B) and red points (C and D). D1-D4) scatterplot of $PM_{2.5}$ and PM_{10} data highlighting valid data (black circle), invalid PM_{10} data (red circle) and reconstructed PM_{10} data (green circle). E1-E4) reconstructed versus measured PM_{10} data.

https://doi.org/10.5194/egusphere-2023-3083
Preprint. Discussion started: 23 February 2024

In our database, we replaced the PM_{10} saturated data by the new PM_{10} re-constructed data, i.e. the red (saturated) points shown in Fig. 3C were replaced by the green re-constructed points. At each site (AQMS), the consistency of the reconstructed data was assessed by analysing the scatter plot of the $PM_{2.5}$ versus PM_{10} data (Fig. 3D1-3D4). As example, the results obtained in AQMSs located in Almería province (Mediterraneo AQMS) and Murcia (Mompean AQMS) in south-eastern Spain, Salamanca province (Salamanca-6 AQMS) in central northern Spain, and in Fuerteventura (Canary Islands) (Fig. 3D1-3D4) is shown (Fig.3D1-3D4). With this method, the red PM_{10}-saturated data shown in Fig. 3D1-3D4 were replaced by the green (reconstructed) data.

Because of the technical manufacturing specification the automatic PM_{10} and $PM_{2.5}$ monitors of four AQMSs were able to record valid and consistent PM_{10} and $PM_{2.5}$ data higher than 1000 $\mu g/m^3$. We used these records to validate this methodology (Fig.3E1, 3E2 and 3E4). At these sites, we re-constructed the PM_{10} concentrations above 1000 $\mu g/m^3$ as if they had experienced saturation and then we compared the "reconstructed versus the measured PM_{10} concentrations"; for this comparison we also included data between 500 and 1000 $\mu g/m^3$ for the purpose of having a larger dataset (i.e. all PM_{10} data > 500 $\mu g/m^3$). We found that the difference between re-constructed and measured PM_{10} concentrations ranged between 2 and 9% (Fig.3E1-3E4). In other few AQMSs using beta attenuation devices able to provide PM_{10} > 1000 $\mu g/m^3$, we found a low PM_{10} variability above this threshold (indicating loos of sensitivity due to mass overload in the filter tape) that was inconsistent with the variability in $PM_{2.5}$ and that resulted in $PM_{2.5}/PM_{10}$ ratios similar to those affected by the saturation as described above (red circles in Fig.3A); at these sites we also reconstructed the PM_{10} with the duxt-r method (Fig.3). Finally, the PM_{10} data measured with the automatic monitors (measured + reconstructed) were converted to gravimetric equivalent data by intercomparison with PM_{10} data obtained with the gravimetric reference method (EN 12341:2015; 24h sampling, available during 7 to 25 days/month depending on the AQMS) using the standardised procedure (EN-16450:2017).

The new dataset obtained with this duxt-r method (PM_{10} measured + reconstructed and then converted to gravimetric equivalent) evidences that 1-hour average PM_{10} data that appeared as "saturated" at 1000 $\mu g/m^3$ actually reached values close to 6000 $\mu g/m^3$ in the dx-02 event, close to 2000 $\mu g/m^3$ in the events dx-01, dx-04 and dx-05, and between 3000 and 4500 $\mu g/m^3$ in the events dx-06 (Fig.2C1-2C3).

By applying this methodology, we reconstructed a total of 1414 hourly PM_{10} data of 48 AQMSs belonging to the regions of Canary Islands (39), Andalucía (5), Murcia (1) and Castilla y León (2) and Madrid (2). The data we reconstructed with this method are already available in public data bases of the Governmental Air Quality Networks of Spain, the Ministry of Ecological Transition and the European Environment Agency. The PM_{10} data of other 44 AQMSs that also experienced PM_{10} saturation could not be reconstructed due to the lack of simultaneous $PM_{2.5}$ measurements, a total of 655 hourly data in these AQMSs located in the Canary Islands (14), Andalucía (10), Extremadura (2), Castilla y León (11) and Murcia (7). Just to

https://doi.org/10.5194/egusphere-2023-3083
Preprint. Discussion started: 23 February 2024

illustrate the huge importance of re-constructing the data, a brief comparison (for a few AQMS) of the 24h average PM_{10} concentrations calculated with saturated PM_{10} data vs reconstructed PM_{10} data: (1) 948 vs 3069 μg/m^3 15 March 2022 in Almería province (Mediterraneo AQMS), (2) 740 vs 1840 μg/m^3 23 feb 2020 in Gran Canaria (Playa del Inglés AQMS), (3) 1238 vs 1684 μg/m^3 23 February 2020 in Tenerife (Tomé Cano AQMS, affected by filter mass overload), (4) 577 vs 1421 μg/m^3 23 February 2020 in Tenerife (Piscina Municipal AQMS), (5) 527 vs 621 μg/m^3 15 March 2022 in Granada province (Palacio de Congresos AQMS).

3.2 The extreme dust events

The six duxt events occurred between February 2020 and March 2022. Four of these episodes affected both the Canary Islands (off NW Africa) and mainland Spain (SW Europe), whereas two of them only affected to the Canaries.

The first two events occurred in February 2020 (Fig.4): 3-5 Feb 2020 (dx-01; Fig.4A1) and 22-29 Feb 2020 (dx-02; Fig.4A2). Throughout six weeks (from mid-January to ending February) a blocking anticyclone established over Iberia, i.e. the Iberian Peninsula (Fig. 4E and 4G), resulting in anomalous easterly wind over central Algeria (wind anomaly not shown for the sake of brevity), a scenario favourable to dust events (Alonso-Pérez et al., 2011a). On 3-5 Feb 2020 a cyclone reached Cape Verde, the low (over Cabo Verde) to high (over Iberia) L-to-H dipole configuration (Fig.4E) resulted in a strong pressure/geopotential gradient and winds that prompted dust emissions and a dense plume of Saharan dust that expanded over the Atlantic to the Canary Islands and the Azores (Fig.4F). Across the Canary Islands the dx-01 event resulted in (i) 1h average PM_{10} and $PM_{2.5}$ concentrations within the range 500-2100 μg/m^3 (Fig.2C1) and 100-560 μg/m^3 (Fig.2B1), respectively, and (ii) 24h average PM_{10} and $PM_{2.5}$ concentrations within the range 200-535^x μg/m^3 (Fig.4A1; Fig.5A1; ^{x} = maximum at Tenerife, San Miguel Tajao AQMS) and 50-165^x μg/m^3 (Fig.4A2; Fig.5A2) (^{x}Tenerife, Tomé Cano AQMS), respectively. Dust events prompted by the summer North African dipole (NAFDI) was originally introduced by Rodríguez et al. (2015). This concept of meteorological L-to-H dipoles has also been found to drive dust events in the Middle East (Kaskaoutis et al., 2015, 2017) and in the June 2020 Godzilla duxt event (Francis et al., 2020).

On 22 Feb 2020, a new cyclone reached again the region of Cape Verde, resulting in a similar L-to-H dipole meteorology (Fig.4G) which prompted a dusty jet stream over the Canary Islands (Fig.4A2, 4H and 4I) and the subtropical North Atlantic. This scenario caused the dark oranges skies, record breaking temperatures, wildfires linked to strong dry winds, closure of maritime and air navigation space and the massive (thousands) flight cancellations described above (Fig.1)(Cuevas et al., 2021). During this dx-02 event, extreme PM_x concentrations were recorded in the Canary Islands, with: (i) 1h average PM_{10} and $PM_{2.5}$ concentrations within the range 2000-5254^x μg/m^3 (Fig.2C1) (^{x}Gran Canaria, Arinaga AQMS) and 400-1129^x μg/m^3 (^{x}Gran Canaria, Mercado Central AQMS) (Fig.2B1), respectively, and (ii) 24h average PM_{10} and $PM_{2.5}$ concentrations

https://doi.org/10.5194/egusphere-2023-3083
Preprint. Discussion started: 23 February 2024

within the range 600-1840[x] μg/m^3 (Fig.4B1, 5B1) ([x]Gran Canaria, Playa del Inglés AQMS) and 200-404[x] μg/m^3 (Fig.4B2, 5B2) ([x]Gran Canaria, Playa del Inglés AQMS), respectively. Concentrations (24h average) of PM_{10} during this dx-02 event were up to 6 times higher than the upper limit of PM_{10} during the regular dust events in the Canary Islands (≈300 μg/m^3) and also much higher than the extraordinary 680 μg/m^3 recorded during the dust event of 26 January 2000 (Viana et al., 2002). During this dx-02 episode, the highest (24-h average) PM_{10} (1200-1840 μg/m^3) and $PM_{2.5}$ (230-404 μg/m^3) concentrations were recorded in the AQMSs located in the central part of the dust plume (Fig.5B1-5B2). After 24 Feb 2020 the Saharan dust plume shifted northward over the Atlantic reaching northern Spain (Fig.4J), resulting in (24h average) PM_{10} and $PM_{2.5}$ concentrations within the range 70-155 μg/m^3 (Fig.4C1) and 20-33 μg/m^3 (Fig.4C2) in central Spain (Madrid, Extremadura and Castilla La Mancha regions) and (24h average) PM_{10} concentrations within the range 80-200 μg/m^3 in eastern Spain (Comunidad Valenciana region) (Fig.4D), respectively. The re-analysis of MERRA-2 properly tracked these two dx-01 & dx-02 events, with dust and $dust_{2.5}$ (i.e. dust in the $PM_{2.5}$ fraction) within the range of the PM_{10} and $PM_{2.5}$ concentrations recorded in the AQMS (see orange circles in Figure 4B-4D).

The third duxt event (dx-03: 15-21 Feb 2021) (Fig.6D) was also caused by the intense wind (Fig.6C) linked a dipole L-to-H meteorology (Fig.6B), with the associated blocking anticyclone located over Iberia and a cyclone over the Sahel (Fig.6B). The impact on the Canary Islands occurred during 15-19 Feb 2021 (Fig.6C); the 16 Feb 2021 resulted in 24h average PM_{10} and $PM_{2.5}$ concentrations within the range 400-638[x] μg/m^3 (Fig.6A1)([x]Las Galletas AQMS, Tenerife) and 80-205[x] μg/m^3 (Fig.6A2)([x]Las Galanas, La Gomera), respectively. On 16 Feb 2021, the highest PM_{10} (> 480μg/m^3) and $PM_{2.5}$ (>120μg/m^3) concentrations were recorded on the western side of the Canary Islands (Fig. 5C1-5C2). Subsequently, the dusty air mass tracked the northward anticyclonic circulation, reaching mainland Spain (18-21 Feb 2021; Fig.6E) and resulting in 24h average PM_{10} and $PM_{2.5}$ concentrations within the range 75-150 μg/m^3 (Fig.6A3) and 20-55 μg/m^3 (Fig.6A4) in Madrid region, respectively. The MERRA-2 reanalysis properly tracked the dx-03 event, except during the 21 of Feb, when it clearly over estimated dust concentrations in central mainland Spain (see orange circles in Figure 6A1-6A4). A few days later, 23-28 Feb 2021, another dust event impacted across central to northern and eastern Europe due to eastward shift the L-to-H dipole and the resulting northward dust transport across the central Mediterranean (Meinander et al., 2023; Peshev et al., 2023).

https://doi.org/10.5194/egusphere-2023-3083
Preprint. Discussion started: 23 February 2024

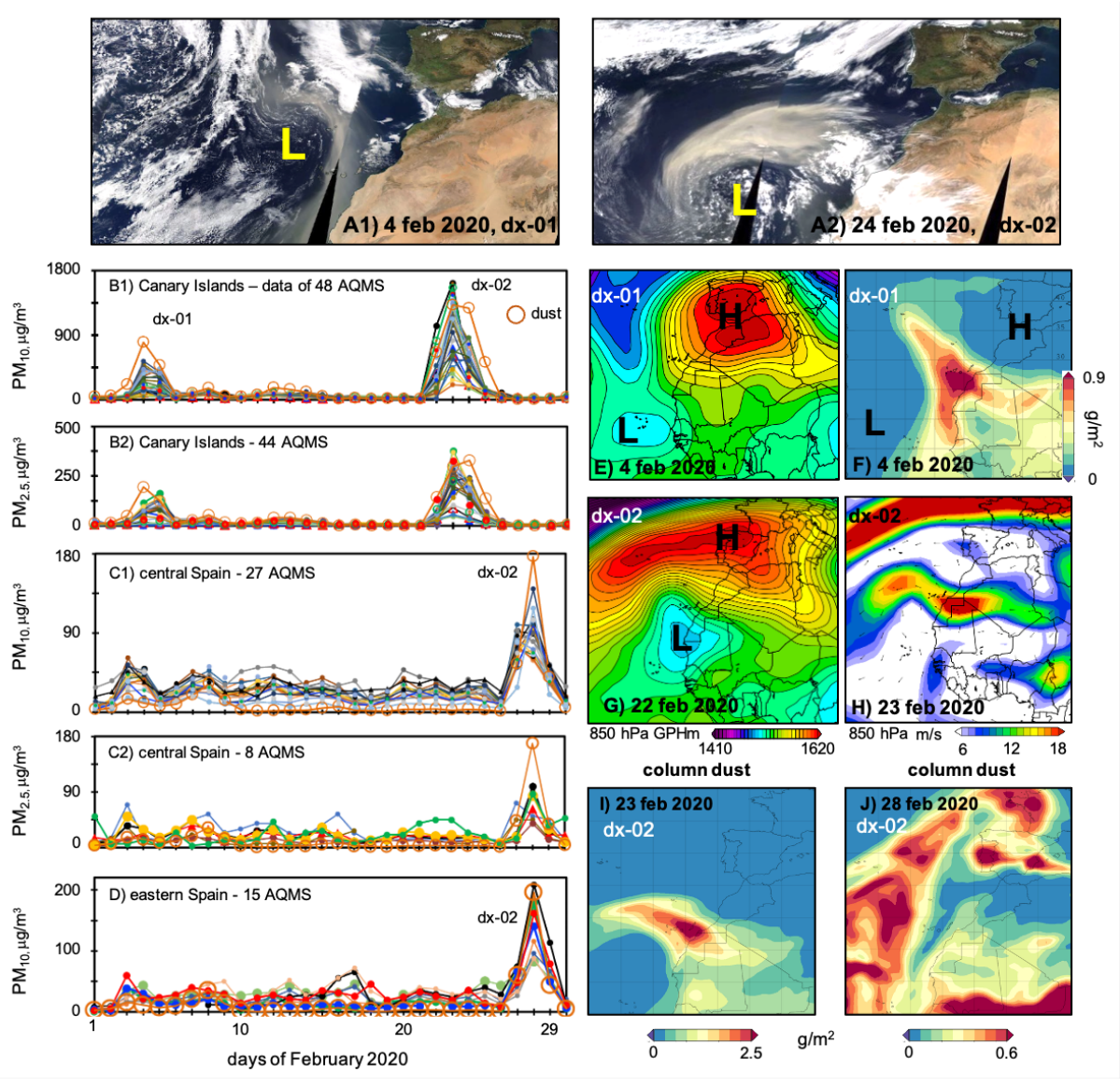

Figure 4. Events dx-01 and dx-02. Satellite view (NOAA-20 VIIRS) of the dust plume during the first day of dx-01 (A1) and dx-02 (A2) events. Time series of 24h average PM_{10} and $PM_{2.5}$ data recorded in AQMSs of the Canary Islands (B1-B2), central Spain (C1-C2) and eastern Spain (D), which includes dust and $dust_{2.5}$ concentrations (µg/m^3) obtained with MERRA-2 model (orange circle) in each region (27-29ºN, 15-17.5ºW domain for the Canary Islands, 39-41ºN, 6.8-4.3ºW for central Spain and 37-41.5ºN, 6.8ºW-1.2ºE for eastern Spain). The geopotential height (GPH) of the 850hPa is shown for the first day of dx-01 (E) and dx-2 (G) events. Wind vector at 850hPa for the 23 Feb 2020 dx-02 (E). MERRA-2 column dust load for the 04 Feb 2020 (F), 23 Feb 2020 (I) and 28 Feb 2020 (J).

https://doi.org/10.5194/egusphere-2023-3083
Preprint. Discussion started: 23 February 2024

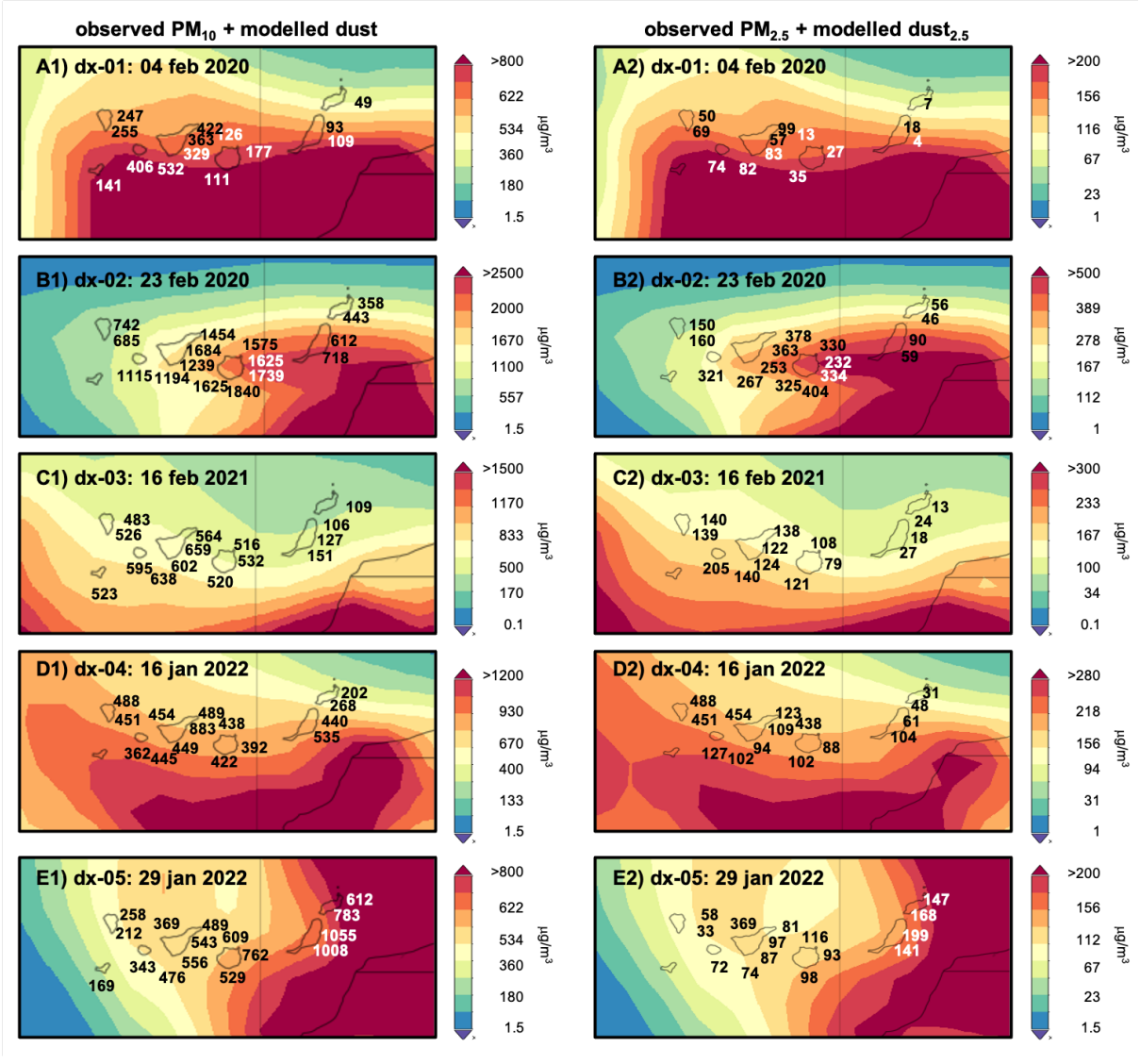

Figure 5. Surface dust and dust$_{2.5}$ concentrations of MERRA-2 reanalysis (26.5-30.0ºN, 19.3-12.0ºW) and observed (24h average) PM$_{10}$ and PM$_{2.5}$ measured in AQMS during specific days of dx-01, dx-02, dx-03, dx-04 and dx-05 events in the Canary Islands.

https://doi.org/10.5194/egusphere-2023-3083
Preprint. Discussion started: 23 February 2024

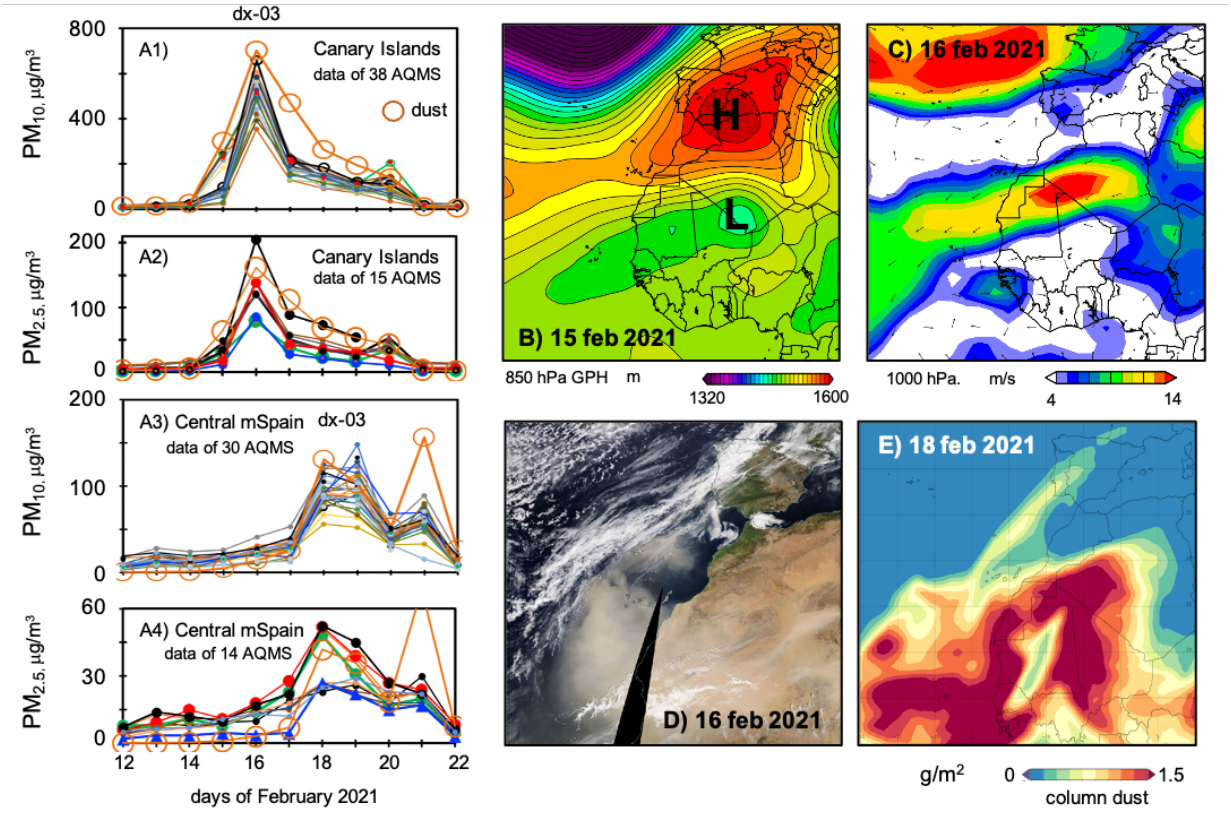

Figure 6. Event dx-03. Time series of (24h average) PM_{10} and $PM_{2.5}$ in AQMSs of the Canary Islands and central mainland Spain (mSpain) and dust and $dust_{2.5}$ concentrations (µg/m^3) obtained with MERRA-2 in the Canary Islands (27-29ºN, 15-17.5ºW) and central mainland Spain (39-41ºN, 6.8-4.3ºW). The geopotential height (GPH) of the 850hPa level (B), wind at 1000hPa (C), the satellite image (NOAA-20 VIIRS)(D) and the column dust load (E) are included.

Another two extreme dust events occurred in January 2022 (Fig.7). The dx-04 event impacted on the Canary Islands during 14-17 Jan 2022, resulting in (24h average) PM_{10} and $PM_{2.5}$ concentrations within the range 275-883^x µg/m^3 (Fig.7A1; Fig.5D1)(^{x}Tenerife, Casa Cuna AQMS) and 60-136^x µg/m^3 (Fig.7A2; Fig.5D2) (^{x}Tenerife, Caletilla AQMS), respectively. A few days later, the dx-05 occurred (29 Jan - 1 Feb 2022) impacting again the Canary Islands, resulting in (24h average) PM_{10} and $PM_{2.5}$ concentrations within the range 314-1055^x µg/m^3 (Fig.7A1; Fig.5E1)(^{x}Fuerteventura, El Charco AQMS) and 70-199^x µg/m^3 (Fig.7A2; Fig.5E2) (^{x}El Charco AQMS), respectively. In both cases a massive dust plume was transported northward, approaching to Spain and Portugal (Fig.7D1-7D2). As in the previous cases, these duxt episodes were caused by a L-to-H dipole meteorology, with an anticyclonic core over Europe expanding to North Africa and a cyclone south of the Canary Islands (Fig.7C1-7C2). In the two events, MERRA-2 clearly overestimated dust concentrations (Fig.7B1-7B2).

https://doi.org/10.5194/egusphere-2023-3083
Preprint. Discussion started: 23 February 2024

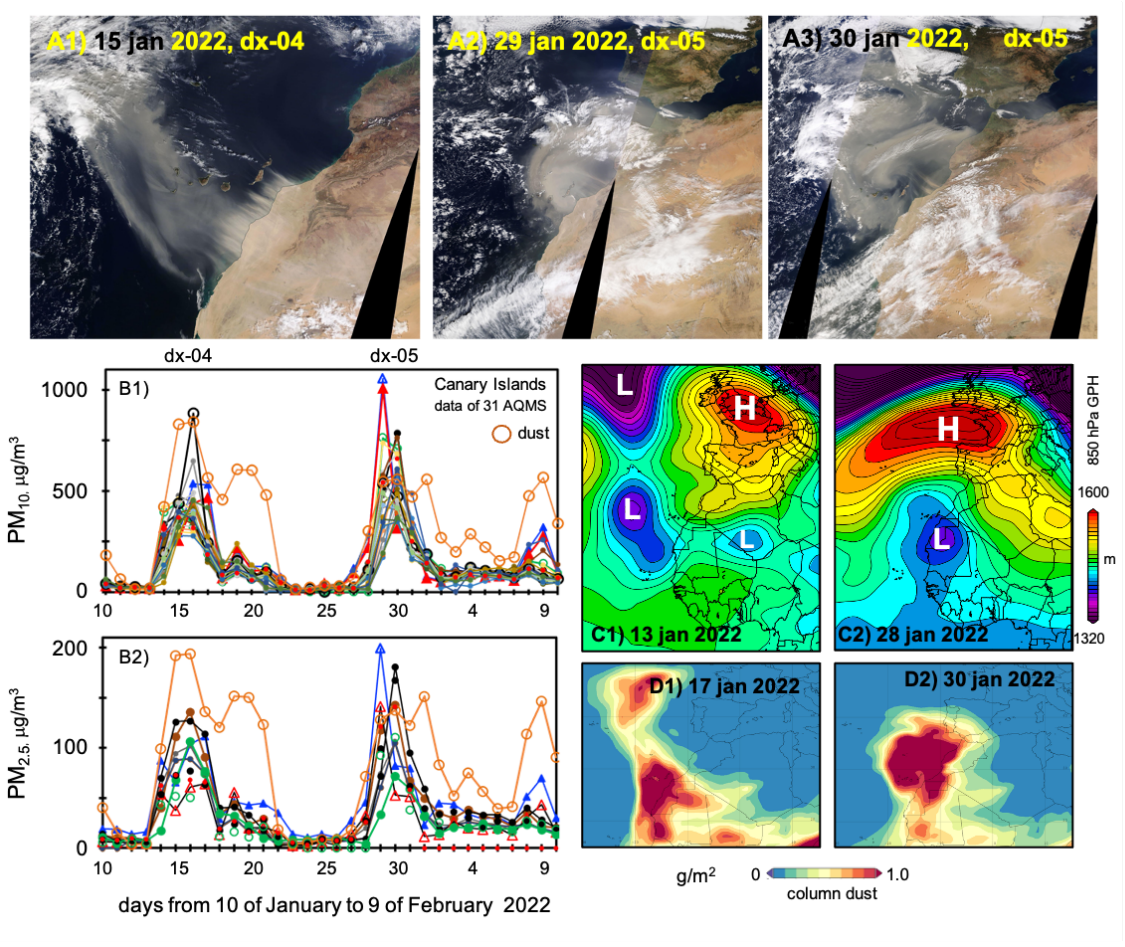

Figure 7. Events dx-04 and dx-05. Satellite view (NOAA-20 VIIRS) of the dust plumes (A1-A3). Time series of (24h average) PM_{10} and $PM_{2.5}$ in AQMSs of the Canary Islands (B1-B2) and MERRA-2 surface dust and $dust_{2.5}$ concentrations in the Canary Islands (27-29ºN, 15-17.5ºW). The geopotential height (GPH) of the 850hPa level (C1-C2) and column dust load (D1-D2) are included.

Finally, the sixth duxt event (dx-06: 15-20 March 2022) first impacted mainland Spain and subsequently the Canary Islands (Fig.8). The event was also prompted by a meteorological L-to-H dipole, linked to the location of the cyclone *Celia* over Morocco and an anticyclonic core over the central Mediterranean (Fig. 8B). The resulting dusty jet (Fig. 8C-8E) expanded from southeast to northwest mainland Spain on the 15 and 16 March 2022. Once in northern Spain, the dust plume split in two branches, a branch travelled eastward across central Europe tracking the anticyclonic circulation at the north of the high-H (Qor-El-Aine et al., 2022), the other branch travelled southward to the Canary Islands tracking the cyclonic L circulation (Fig.8E-8F).

https://doi.org/10.5194/egusphere-2023-3083
Preprint. Discussion started: 23 February 2024

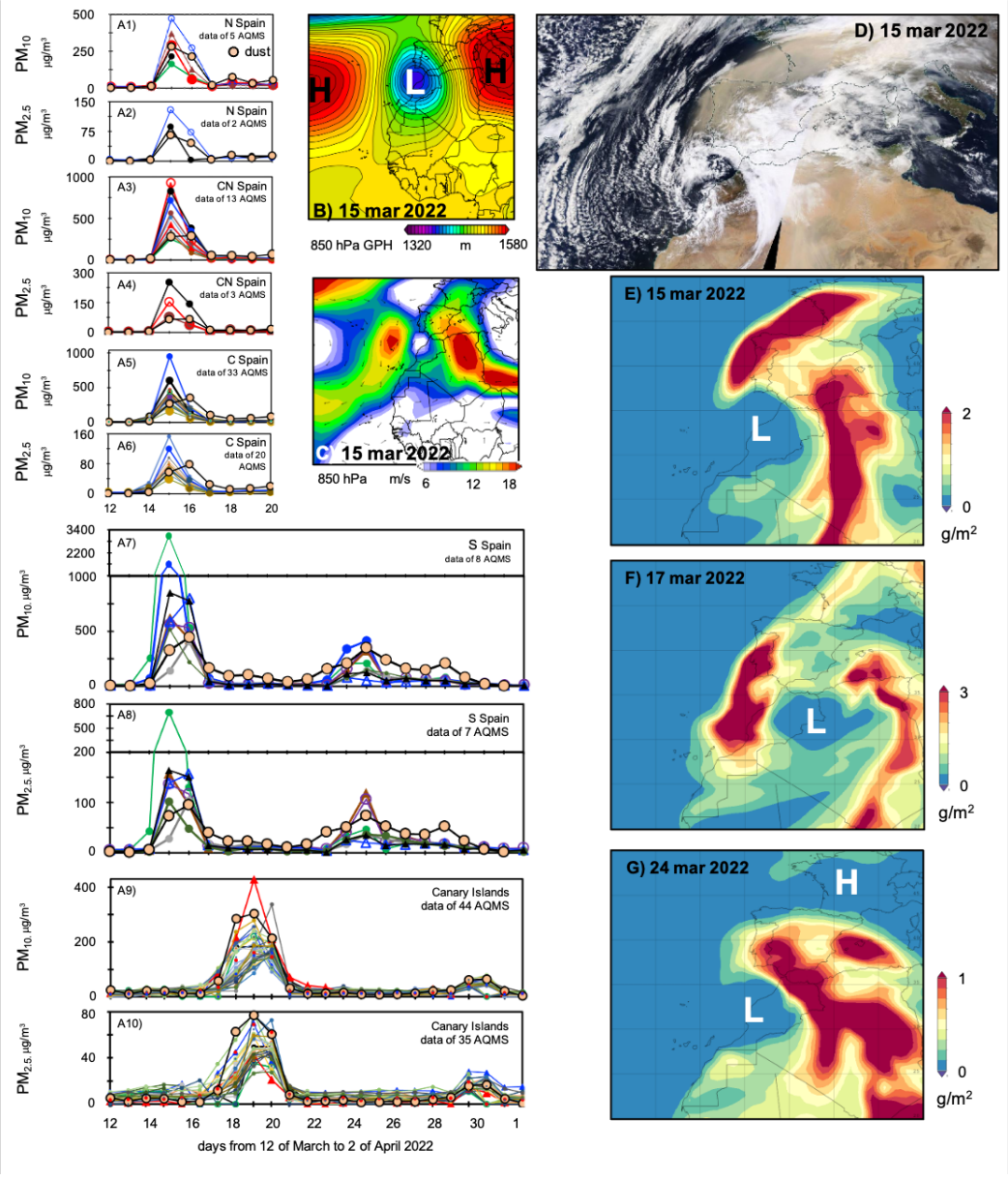

Figure 8. Event dx-06. Time series of (24h average) PM_{10} and $PM_{2.5}$ in AQMSs in of Northern (N) (A1-A2: Cantabria and Galicia regions), central-north (CN) (A3-A4: Castilla y León region), central (C) (A5-A6: Madrid + Extremadura + Castilla La Mancha regions) and southern (S) (A7-A8, Andalucía region) mainland Spain and in the Canary Islands (A9-A10). The plots also include surface dust concentrations in these regions obtained with MERRA-2 reanalysis (A1-A10). The geopotential height (GPH) (B) and wind (C) in the 850hPa level, the satellite NOAA-20 VIIRS image and column dust load (E-G) is also included.

https://doi.org/10.5194/egusphere-2023-3083
Preprint. Discussion started: 23 February 2024

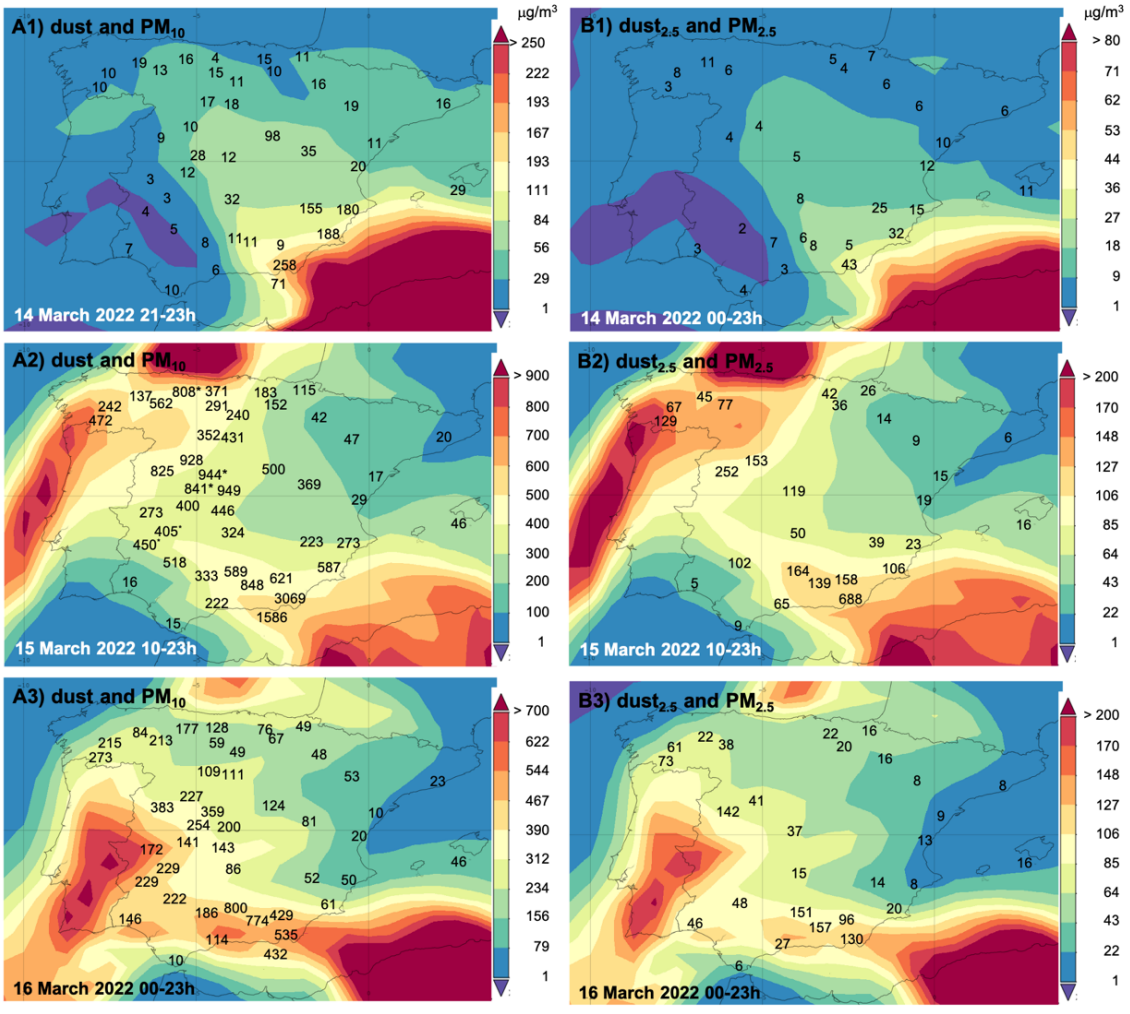

Figure 9. Surface concentrations of dust (A1-A3) and dust particles smaller than 2.5 microns ($dust_{2.5}$) (B1-B3) from 14 to 16 March 2022 in mainland Spain according to MERRA-2 reanalysis. Daily (24h) average concentrations of PM_{10} (A1-A2) and $PM_{2.5}$ (B1-B2) measured in AQMSs are shown with black numbers.

https://doi.org/10.5194/egusphere-2023-3083
Preprint. Discussion started: 23 February 2024

In mainland Spain, PM_x concentrations experienced a sharp increase, from their regular background levels (10-30 $\mu g/m^3$) to 24h average PM_{10} and $PM_{2.5}$ values within the range (i) 500-3060 $\mu g/m^3$ (Fig.8A7) and 100-700 $\mu g/m^3$ (Fig.8A8) in southern Spain (Andalucía and Murcia regions), (ii) 200-1000 $\mu g/m^3$ (Fig.8A5) and 60-160 $\mu g/m^3$ (Fig.8A6) in central Spain (Castilla La Mancha, Madrid and Extremadura regions), (iii) 200-1000 $\mu g/m^3$ (Fig.8A3) and 60-260 $\mu g/m^3$ (Fig.8A4) in central northern Spain (Castilla y León region), and (iv) 150-500 $\mu g/m^3$ (Fig.8A1) and 75-130 $\mu g/m^3$ (Fig.8A2) in northern Spain (Cantabria and Galicia regions) during the 15-16 March 2022, respectively. After several days traveling across thousands of kilometres, the dust plume impacted in the Canary Islands during 17-20 March 2022 (Fig.8F), resulting in (24h average) PM_{10} and $PM_{2.5}$ values within the range 150-430 $\mu g/m^3$ (Fig.8A9) and 30-80 $\mu g/m^3$ (Fig.8A10). A regular (no extreme) dust event impacted southern Spain 24-25 March 2022 (PM_{10} and $PM_{2.5}$: 50-420 $\mu g/m^3$ and 30-120 $\mu g/m^3$; respectively) (Fig.8A7-8A8) and the Canary Islands 24-25 March 2022 (PM_{10} and $PM_{2.5}$: 40-80 and 20-35 $\mu g/m^3$, respectively).

This historic dx-06 event (Fig.1D-1E) started the evening of 14 March 2022 (>21h), with a dust inflow in south-eastern Spain that led to 24h average PM_{10} and $PM_{2.5}$ concentrations within the range 70-260 $\mu g/m^3$ and 25-43 $\mu g/m^3$ (Fig.9A1-9B1). On 15 March 2022, mainland Spain was blanketed by the massive dusty airmass (Fig.9A2-9B2), which led to 24h average PM_{10} values of: (i) 3069 $\mu g/m^3$ (Mediterraneo AQMS; Almería province), 1586 $\mu g/m^3$ (El Ejido; Almería), 848 $\mu g/m^3$ (Ronda del Valle; Jaén), 621 $\mu g/m^3$ (Palacio de Congresos; Granada) and 587 $\mu g/m^3$ (Mompean; Murcia) in south-eastern Spain and 518 $\mu g/m^3$ in central southern Spain (Sierra Norte; Seville), (ii) 949 $\mu g/m^3$ (Villa del Prado; Madrid), 944* $\mu g/m^3$ (Segovia-2; Segovia), 928 $\mu g/m^3$ (Medina del Campo; Valladolid), 841* $\mu g/m^3$ (Avila-II; Avila) and 825 $\mu g/m^3$ (Salamanca-6; Salamanca) in central Spain, and (iii) 808* $\mu g/m^3$ (Lario; León), 562 $\mu g/m^3$ (León-01; León), 472 $\mu g/m^3$ (Laza; Orense) and 371 $\mu g/m^3$ (Los Tojos; Cantabria) in Norwest Spain (Fig.9A2). Some of these PM_{10} concentrations (highlighted with asterisk*) are actually slightly underestimated due to the automatic PM_{10} monitor reached the saturation level (1000 $\mu g/m^3$) during a few hours and the *duxt-r* reconstruction method could not be applied to the lack of parallel $PM_{2.5}$ data. On 15 March 2022, the 24h average $PM_{2.5}$ values reached values of (Fig.9B2): (i) 688 $\mu g/m^3$ (Mediterraneo; Almería), 164 $\mu g/m^3$ (Ronda del Valle; Jaén), 158 $\mu g/m^3$ (Palacio de Congresos; Granada) in south-eastern Spain, (ii) 252 $\mu g/m^3$ (Salamanca-6), 153 $\mu g/m^3$ (Medina del Campo; Valladolid) and 119 $\mu g/m^3$ (Villa del Prado; Madrid) in central Spain and (iii) 129 $\mu g/m^3$ (Laza; Orense) in north-west Spain. During the 16 March 2022, high PM_{10} and $PM_{2.5}$ values were still recorded (Fig.9A3-9B3), with the highest PM_{10} concentrations linked to the still ongoing dust inflow by south-eastern Spain: 800 $\mu g/m^3$ (Bailén; Jaén), 774 $\mu g/m^3$ (Ronda del Valle; Jaén), 535 $\mu g/m^3$ (Mediterraneo; Almería) and 432 $\mu g/m^3$ (El Ejido; Almería). During the dx-06 event, the hourly PM_{10} concentrations exceeded 2000 $\mu g/m^3$ at four sites which reached maximum PM_{10} values: >4573* $\mu g/m^3$ (Mediterraneo; Almería), 3502 $\mu g/m^3$ (El Ejido; Almería), 2813 $\mu g/m^3$ (Mompean; Murcia) and 2154 $\mu g/m^3$ (Ronda del Valle; Jaén) (Fig.2C3). Similarly, the hourly values of $PM_{2.5}$ exceeded 400 $\mu g/m^3$ at four sites, where the maximum 1h $PM_{2.5}$ concentration were:

https://doi.org/10.5194/egusphere-2023-3083
Preprint. Discussion started: 23 February 2024

1000* μg/m^3 (Mediterraneo; Almería, $PM_{2.5}$ analyzer saturated), 471 μg/m^3 (Mompean; Murcia), 443 μg/m^3 (Salamanca-6), 400 (Ronda del Valle; Jaén). On 15 March, hourly $PM_{2.5}$ concentrations at Mediterraneo AQMS saturated at 1000 μg/m^3 during 6 hours (08-13h), so the daily average $PM_{2.5}$ value = 688 μg/m^3 at this site is actually somewhat underestimated and consequently also the daily average PM_{10} value = 3069 μg/m^3 (obtained with the duxt-r method).

3.3 Record breaking events

The analysis of the 2000-2022 time series of (24h average) PM_{10} (Fig.10) and $PM_{2.5}$ (Fig.11) data, evidence that the duxt events we report here are record beating episodes in Spain, both for mainland Spain and the Canary Islands. The massive dusty airmass that blackened mainland Spain during the 15 and 16 of March 2022 (dx-06; Fig.10 and 11) resulted in the highest PM_{10} and $PM_{2.5}$ concentrations ever recorded in the regional scale across northern Spain (Cantabria region; Fig.10A), central -northern Spain (Castilla y León region; Fig. 10C & 11A), central Spain (Castilla La Mancha, Extremadura and Madrid region; Fig.10D & 10A) and southern Spain (Andalucía region; Fig. 10E, 10F & 11C). For example, in central Spain (Castilla La Macha + Extremadura + Madrid), regular Saharan dust events typically induce (24h average) PM_{10} concentrations within the range 40-140 μg/m^3 (highlighted with black arrows in Fig.10D) (Pey et al., 2013; Rodríguez et al., 2001), whereas during the dx-06 event 33 AQMSs of this region recorded (24h average) PM_{10} concentration within 300-949^x μg/m^3 (^{x}Villa del Prado AQMS in Madrid region)(white arrow in Fig. 10D). After analysing the 2001-2011 time series, Pey et al.(2013) concluded that in the Western Mediterranean, Saharan dust events inducing PM_{10} >100 μg/m^3 (24h average) are actually rare. The impact of the dx-06 event is not observed in Cataluña since it did not reach Northeast Spain (Fig.10B).

https://doi.org/10.5194/egusphere-2023-3083
Preprint. Discussion started: 23 February 2024

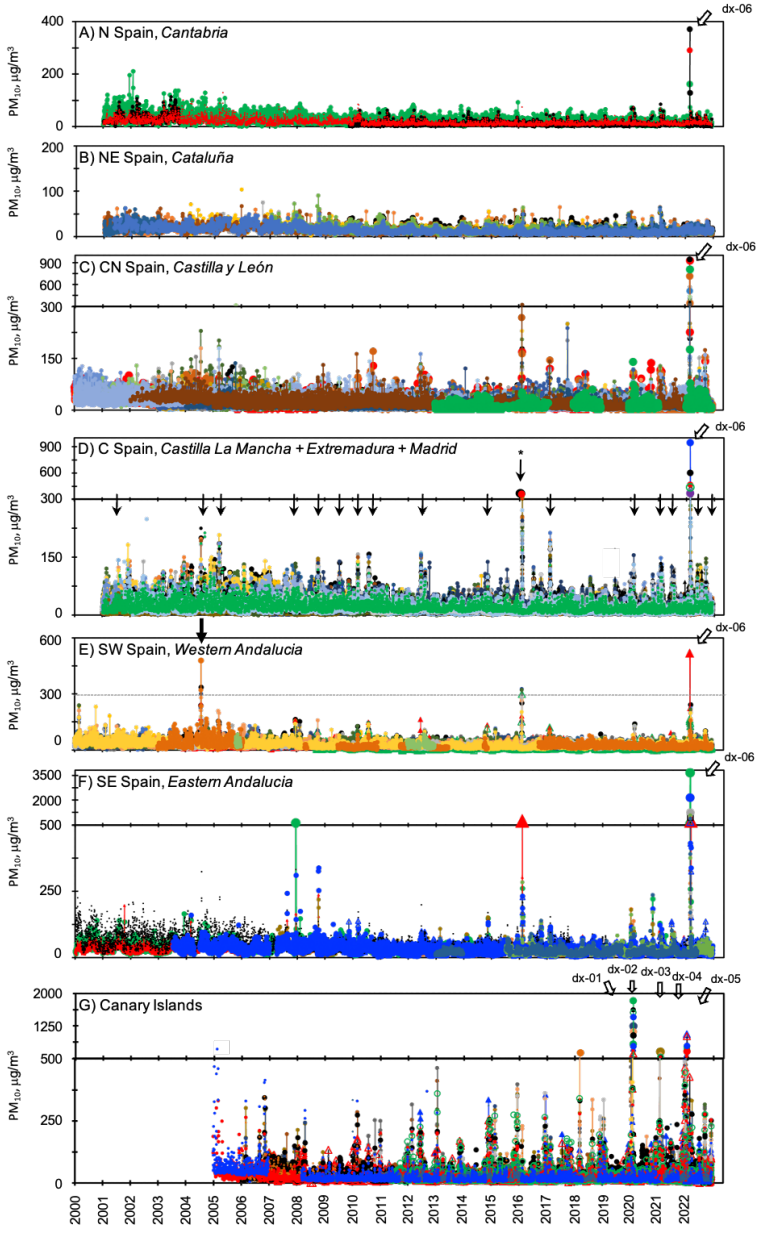

Figure 10. Time series (2000-2022) of (24h average) PM_{10} concentrations of 118 AQMSs distributed across northern (N; 3 AQMSs), North-East (NE; 8 AQMSs), Central-North (CN; 30 AQMSs), Central (C; 35 AQMSs), Southwest (SW; 16 AQMSs) and Southeast (SE; 11 AQMSs) mainland Spain and in the Canary Islands (15 stations). Black arrows indicate regular dust events. White arrows indicate the duxt events. The asterisk indicates the intense event occurred 22 Feb 2016.

https://doi.org/10.5194/egusphere-2023-3083
Preprint. Discussion started: 23 February 2024

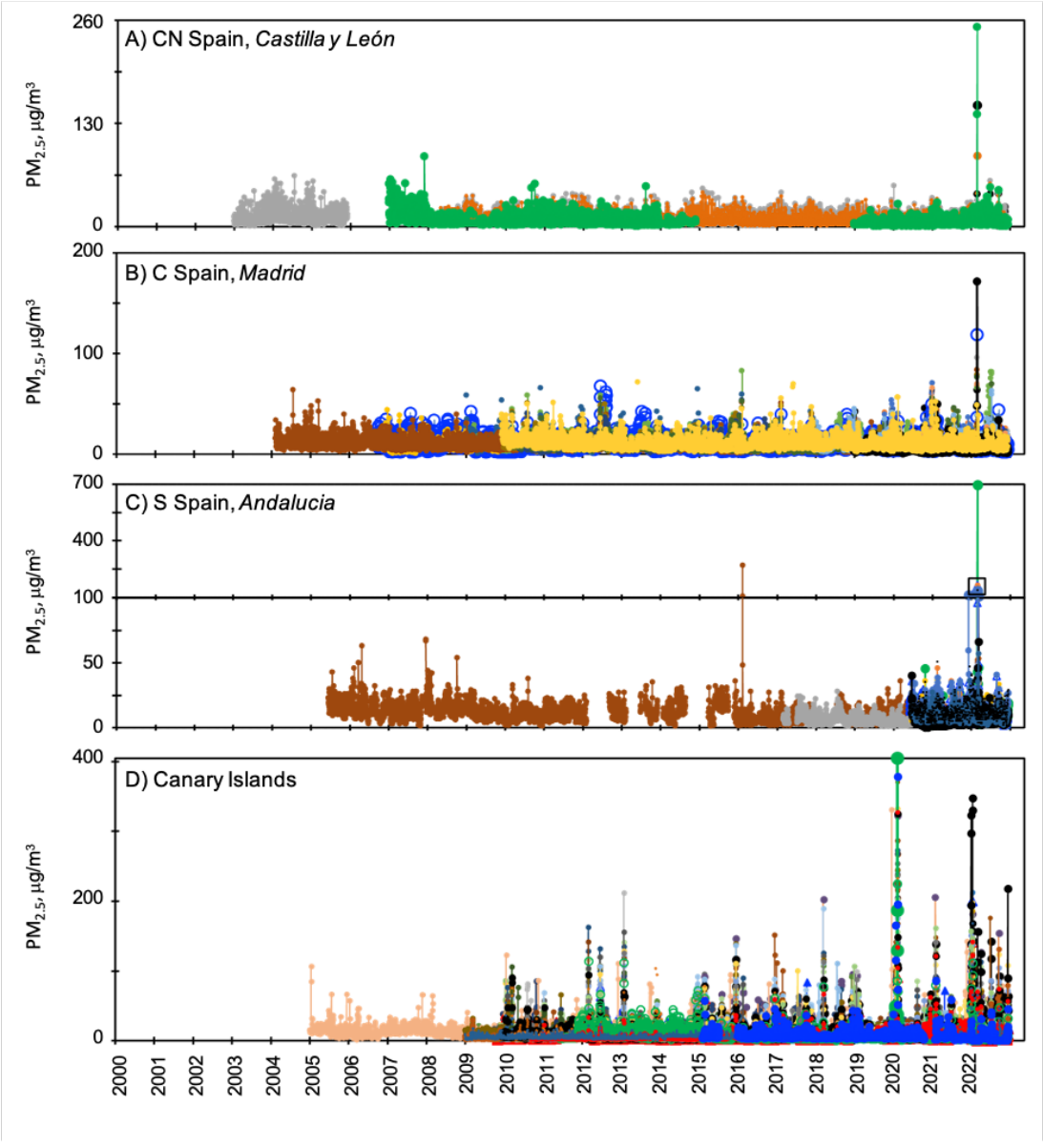

Figure 11. Time series (2000-2022) of (24h average) $PM_{2.5}$ concentrations of in a total of 74 AQMSs distributed across the Central-North (CN; 4 AQMSs), Central (C; 16 AQMSs) and Southeast (S; 10 AQMSs) mainland Spain and in the Canary Islands (44 stations). Black arrows indicate regular dust events. White arrows indicate the duxt events.

https://doi.org/10.5194/egusphere-2023-3083
Preprint. Discussion started: 23 February 2024

In the Canary Islands, the most intense Saharan dust events ever recorded occurred in the period 2020-2022 linked to the duxt events described in this study. Since 2005 to 2020, intense Saharan dust events have regularly been associated with (24h average) PM_{10} and $PM_{2.5}$ values with 200-400 $\mu g/m^3$ (Fig.10G) and 100-200 $\mu g/m^3$ (Fig.10D), respectively. This PM_{10} range is similar to (1) that of total suspended particles during Saharan dust events of the period 1998-2003, based on AQMS data not yet normalised to the European standards (Alonso-Pérez et al., 2007, 2012; Viana et al., 2002), and to (2) that of total dust at Izaña Observatory (Tenerife) during the 1987-2014 Saharan dust events (Rodríguez et al., 2015). In contrast, in the period 2020-2022, the duxt events described here led to PM_{10} and $PM_{2.5}$ concentrations within the ranges 600-1840 $\mu g/m^3$ (Fig.10G) and 200-404 $\mu g/m^3$ (Fig.11D), respectively. The three most intense dust events ever recorded in the Canary Islands, exceeding the threshold of 600 $\mu g/m^3$ of PM_{10} as 24h average, in descending order of magnitude, are:

1. dx-02 event: the 23 and 24 Feb 2020 the (24h average) PM_{10} averaged in all AQMSs were 531 and 930 $\mu g/m^3$ (averages of 34 AQMSs distributed in the 7 Canary Islands), respectively. The 22, 23 and 24 Feb 2020, a total of 6, 25 and 12 AQMSs recorded a (24h average) PM_{10} concentration between 600 and 1840^x $\mu g/m^3$ (^{x}Gran Canaria, Playa del Inglés AQMS). Previous to this event, the (24h average) PM_{10} concentrations had only exceeded 600 $\mu g/m^3$ in just one AQMS (618 $\mu g/m^3$ at Las Galanas during the dust event 28 March 2018; Fig.10G).
2. dx-05 event: 29 and 30 Jan 2022 the (24h average) PM_{10} averaged in all the AQMSs was 463 and 501 $\mu g/m^3$ (averages of 44 AQMSs distributed in the 7 islands). The 29 and 30 of Jan 2022, a total of 9 and 10 AQMSs recorded a (24h average) PM_{10} concentration between 600 and 1055^x $\mu g/m^3$ (^{x}Fuerteventura, El Charco AQMS).
3. dx-03 event: the 16 Feb 2021 the (24h average) PM_{10} averaged in all AQMSs was 463 $\mu g/m^3$ (average of 36 AQMSs distributed in the 7 islands). The 16 Feb 2021, 4 AQMSs recorded a (24h average) PM_{10} concentration between 600 and 638^x $\mu g/m^3$ (^{x}Las Galletas AQMS, Tenerife).

In mainland Spain, the dx-06 is the most intense dust event ever recorded. A total of 20 AQMSs, distributed across south-eastern, central to central-northern Spain, registered (24h average) PM_{10} concentrations within the range 600 to 3069^x $\mu g/m^3$ (^{x}Mediterraneo AQMS in Almería province). The 2 decades time series of PM_x also offer other interesting data. In many of regions of Spain there is a clear 2000-2020 decreasing trend of PM_{10} concentrations linked to the reduction of emissions following air quality policies (Fig.10A, 10C, 10E) (Li et al., 2018; Querol et al., 2014).

https://doi.org/10.5194/egusphere-2023-3083
Preprint. Discussion started: 23 February 2024

3.4 Meteorological anomalies linked to duxt events

The 2020-2022 six duxt events we report here were induced by the L-to-H meteorological dipoles formed by cyclones located at the southwest of a blocking anticyclone over western Europe. Fig. 12 (A1 to F1) show the anomaly of the 500 hPa geopotential height during the onset of the six duxt events studied here (Fig.12 A2 to F2). All duxt events occurred during northern-hemisphere meteorological anomalies that resemble the anomalies of the atmospheric circulation linked to the anthropogenic global warming (Fig.12): (i) subtropical anticyclones intensified and expanded to higher latitudes (Cherchi et al., 2018; Cresswell-Clay et al., 2022), (ii) anomalous low pressures expanding northward beyond the tropical belt, resembling the tropical expansion (Seidel et al., 2008; Yang et al., 2020, 2023) (e.g. dx-01, dx-02, dx-03 and dx-04) and (iii) mid-latitudes amplified undulation of the Rossby waves due to the concatenation of cut-off lows - cyclones and anticyclones pointing to a weakening of the polar vortex (e.g. dx-03, dx-05, dx-06 and 23-mar-2022) (Mann et al., 2017). The duxt events observed at the Eastern Mediterranean in March 2018 (Solomos et al., 2018), at North Africa in June 2020 (Bi et al., 2023; Francis et al., 2020), at Uzbekistan in November 2021 (Xi et al., 2023) and in China in March 2021 (Gui et al., 2022), occurred in this context of cyclones, blocking anticyclones and dipoles linked to mid-latitudes amplified Rossby waves.

The winter blocking anticyclone that we observed over western Europe/Western Mediterranean during the duxt events (Fig.12A1-G1) fits with the picture of the industrial-era eastward expansion of the North Atlantic anticyclone starting in the 1850s and accelerating in the last few decades (Alonso-Pérez et al., 2011b; Cresswell-Clay et al., 2022), a trend that is expected to continue as the concentrations of greenhouses gases increase, according to the CMIP5 multi-model simulations (Cherchi et al., 2018); the low pressures at the southwest of the blocking anticyclone that we observe during the duxt events (Fig.12B1-12E1) are expected to follow as the tropic expands northward off North Africa in the forthcoming decades (e.g. see Fig 1F of Cherchi et al. 2018 for the 2075-2100 period).

The anomalies linked to the duxt events are also evident in the trajectory of the cyclones that finally form the L-to-H dipoles leading to the extreme dust emissions. Red circles in Fig.12A1-12G1 indicate the location of the cyclones from days before (negative number) to days after (positive number) of the duxt event. Due to the anticyclonic blocking over western Europe, the mid-latitudes North Atlantic cyclones didn't follow their regular path across Europe or the Mediterranean. The cut-off lows forming the L-to-H dipoles reached this region (Canary Islands, Cape Verde or inner Sahara) by two main paths:

https://doi.org/10.5194/egusphere-2023-3083
Preprint. Discussion started: 23 February 2024

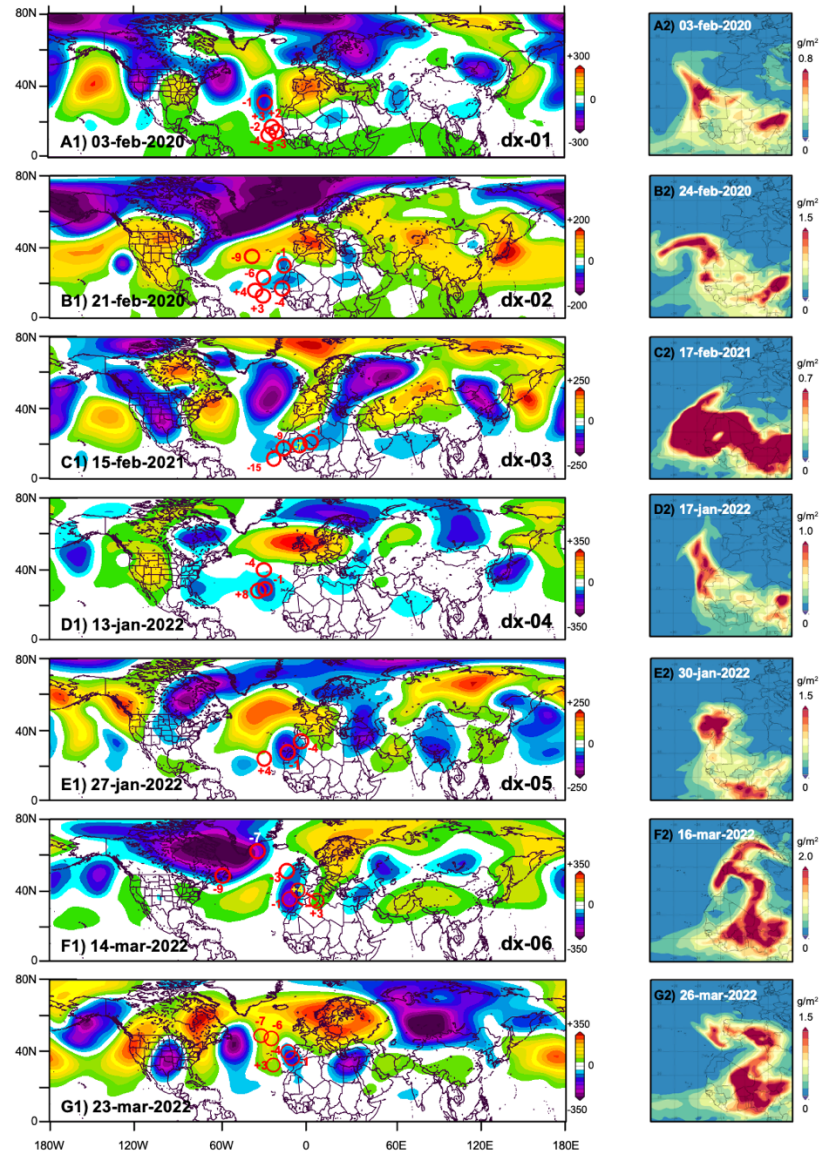

Figure 12. Anomaly (A1-G1) of the 500 hPa geopotential height (GPH) (respect to the 1991-2020 climatology) and column dust in the onset of the dx-01 to dx-06 and 24-26 March 2022 events (A2-G2). Red circles (A1-G1) indicate the location of the cyclones days before (negative number) to days after (positive number) the first day of the duxt event.

https://doi.org/10.5194/egusphere-2023-3083
Preprint. Discussion started: 23 February 2024

1. they deviated southward from the North Atlantic mid-latitudes as results of the blocking anticyclone over western Europe; subsequently these cut-off lows may stay during long periods (up to 12 days) in the subtropical and tropical north-east Atlantic (near the Canary Islands and Cape Verde). This is the case of the dipoles of events dx-02, dx-04, dx-05 and dx-06, and also of the intense dust event of 23 March 2022. The cyclones of the events dx-02, dx-04 and dx-05 stayed (blocked by the anticyclonic situation) near the Canary Islands and Cape Verde during 10, 12 and 8 days (Fig. 12B1, 12D1 and 12E1), respectively.
2. they deviated northward from the tropical belt. This is the case of the events dx-01 and dx-03, associated with cyclones which had moved from Cape Verde to the west of the Canary Islands (Fig.12A1, dx-01) and to the inner Sahara (Fig.12C1, dx-03), respectively, across a tropical band anomalously shifted to northward.

4 Summary and conclusions

In winter 2020, 2021 and 2022 a set of six extreme dust events expanded northward from NW Africa to the Atlantic and Europe, causing extremely high concentrations of PM_{10} and $PM_{2.5}$ in the Governmental Air Quality Monitoring Stations of the Canary Islands and mainland Spain, up to exceeding the upper operation limit of many PM_{10} monitors. We developed the *duxt-r* methodology for assessing the consistency of the PM_{10} and $PM_{2.5}$ data and re-construct the underestimated PM_{10} concentrations. During these extreme dust events, the 1-hour average PM_{10} and $PM_{2.5}$ concentrations were within the range 1000-6000 $\mu g/m^3$ and 400-1200 $\mu g/m^3$, whereas the 24-h average PM_{10} and $PM_{2.5}$ data were within the range 500-3070 $\mu g/m^3$ and 200-690 $\mu g/m^3$, respectively. These extreme dust episodes are caused by the intense winds associated with the meteorological dipoles formed by a blocking anticyclone over western Europe and a cut-off low - cyclone located at the southwest, near the Canary Islands, Cape Verde or into the Sahara. The analysis of the 2000-2022 time series of PM_{10} and $PM_{2.5}$ shows that these events have no precedent in Spain. Record breaking PM_{10} and $PM_{2.5}$ (24h average) concentrations were measured in the Canary Islands during the 22-24 February 2020, 1840 $\mu g/m^3$ and 404 $\mu g/m^3$, and in mainland Spain during 15-16 March 2022, 3069 $\mu g/m^3$ and 688 $\mu g/m^3$ (Almeria province), respectively. All duxt events occurred during northern-hemisphere meteorological anomalies associated with subtropical anticyclones intensified and expanded to higher latitudes, anomalous low pressures expanding beyond the tropical belt and a concatenation of cut-off lows and anticyclones suggesting to a weakening of the polar vortex, with features that resemble the change in the atmospheric circulation linked to climate change. These events occurs in the context in which climate projections forecast the expansion of the North African drylands toward the northwest, increasing the risk of desertification of Spain. The air quality monitoring networks need to adapt the strategy and operation range of the PM_{10} and $PM_{2.5}$ monitoring programs to ensure accurate measurements can be done during

https://doi.org/10.5194/egusphere-2023-3083
Preprint. Discussion started: 23 February 2024

these extreme dust events due to the importance of having suitable data in the public data sets for health effects studies, modelling, etc…

Data availability

The data used in the manuscript are available in public data bases, including the PM_{10} data reconstructed as result of this study. Data are also available by request to the first author at sergio.rodriguez@csic.es

Author contributions

SR and JLD performed the conceptualisation, investigation, data collection, treatment and formal analysis. SR wrote the original version of the manuscript, which was subsequently revised and edited by SR and JLD.

Competing interests

The authors declare that they have no conflict of interest.

Acknowledgments

We thanks to the 12 Autonomous Regions of Spain and the Ministry for the Ecological Transition and the Demographic Challenge for the kind supply to the data of the air quality monitoring stations. We acknowledgement the access to modelling reanalysis data by the portal web sites of NASA - Giovanni and NOAA – Physical Science Laboratory. We also thanks to Jon Vilches (air quality management in the Government of the Canary Islands) for the interesting talks on the PM_x monitoring devices.

Financial support

This study is part of the project AERO-EXTREME (PID2021-125669NB-I00) funded by the funded by the State Research Agency/Agencia Estatal de Investigación of Spain and the European Regional Development Funds.

https://doi.org/10.5194/egusphere-2023-3083
Preprint. Discussion started: 23 February 2024

References

Alonso-Pérez, S., Cuevas, E., Querol, X., Viana, M. and Guerra, J. C.: Impact of the Saharan dust outbreaks on the ambient levels of total suspended particles (TSP) in the marine boundary layer (MBL) of the Subtropical Eastern North Atlantic Ocean, Atmos. Environ., 41(40), 9468–9480, doi:10.1016/j.atmosenv.2007.08.049, 2007.

Alonso-Pérez, S., Cuevas, E. and Querol, X.: Objective identification of synoptic meteorological patterns favouring African dust intrusions into the marine boundary layer of the subtropical eastern north Atlantic region, Meteorol. Atmos. Phys., 113(3–4), 109–124, doi:10.1007/s00703-011-0150-z, 2011a.

Alonso-Pérez, S., Cuevas, E., Perez, C., Querol, X., Baldasano, J. M., Draxler, R. and De Bustos, J. J.: Trend changes of African airmass intrusions in the marine boundary layer over the subtropical Eastern North Atlantic region in winter, Tellus B, 63(2), 255–265, doi:10.1111/j.1600-0889.2010.00524.x, 2011b.

Alonso-Pérez, S., Cuevas, E., Querol, X., Guerra, J. C. and Pérez, C.: African dust source regions for observed dust outbreaks over the Subtropical Eastern North Atlantic region, above 25°N, J. Arid Environ., 78, 100–109, doi:10.1016/j.jaridenv.2011.11.013, 2012.

Bi, H., Chen, S., Zhang, D., Wang, Y., Kang, L., Alam, K., Tang, M., Chen, Y., Zhang, Y. and Wang, D.: The Circum-global Transport of Massive African Dust and its Impacts on the Regional Circulation in Remote Atmosphere, Bull. Am. Meteorol. Soc., doi:10.1175/BAMS-D-23-0072.1, 2023.

Cañadillas-Ramallo, D., Moutaoikil, A., Shephard, L. E. and Guerrero-Lemus, R.: The influence of extreme dust events in the current and future 100% renewable power scenarios in Tenerife, Renew. Energy, 184, 948–959, doi:10.1016/j.renene.2021.12.013, 2022.

Cherchi, A., Ambrizzi, T., Behera, S., Freitas, A. C. V., Morioka, Y. and Zhou, T.: The Response of Subtropical Highs to Climate Change, Curr. Clim. Chang. Reports, 4(4), 371–382, doi:10.1007/s40641-018-0114-1, 2018.

Cresswell-Clay, N., Ummenhofer, C. C., Thatcher, D. L., Wanamaker, A. D., Denniston, R. F., Asmerom, Y. and Polyak, V. J.: Twentieth-century Azores High expansion unprecedented in the past 1,200 years, Nat. Geosci., 15(7), 548–553, doi:10.1038/s41561-022-00971-w, 2022.

Cuevas, E., Milford, C., Barreto, A., Bustos, J. J., García, R. D., Marrero, C. L., Prats, N., Bayo, C., Ramos, R., Terradellas, E., Suárez, D., Rodríguez, S., de la Rosa, J., Vilches, J., Basart, S., Werner, E., López-Villarrubia, E., Rodríguez-Mireles, S., Pita Toledo, M. L., González, O., Belmonte, J., Puigdemunt, R., Lorenzo, J. A., Oromí, P. and del Campo-Hernández, R.: Desert Dust Outbreak in the Canary Islands (February 2020): Assessment and Impacts. (Eds. Cuevas, E., Milford, C. and

https://doi.org/10.5194/egusphere-2023-3083
Preprint. Discussion started: 23 February 2024

Basart, S.), State Meteorological Agency (AEMET), Madrid, Spain and World Meteorological Organization, Geneva, Switzerland, WMO Global At. [online] Available from: http://hdl.handle.net/20.500.11765/12703, 2021.

Cuevas, E., Barriopedro, D., Delia García, R., Alonso-Pérez, S., González-Alemán, J., Werner, E., Suárez, D., Bustos, J., García-Castrillo, G., García, O., Barreto, A. and Basart, S.: Sharp increase of Saharan dust intrusions over the Western Mediterranean and Euro-Atlantic region in winters 2020-2022 and associated atmospheric circulation, Atmos. Chem. Phys. Discuss., doi:https://doi.org/10.5194/egusphere-2023-1749, 2023.

Domínguez-Rodríguez, A., Báez-Ferrer, N., Abreu-González, P., Rodríguez, S., Díaz, R., Avanzas, P. and Hernández-Vaquero, D.: Impact of Desert Dust Events on the Cardiovascular Disease: A Systematic Review and Meta-Analysis, J. Clin. Med., 10(4), 727, doi:10.3390/jcm10040727, 2021.

Dumont, M., Tuzet, F., Gascoin, S., Picard, G., Kutuzov, S., Lafaysse, M., Cluzet, B., Nheili, R. and Painter, T. H.: Accelerated Snow Melt in the Russian Caucasus Mountains After the Saharan Dust Outbreak in March 2018, J. Geophys. Res. Earth Surf., 125(9), doi:10.1029/2020JF005641, 2020.

Evan, A. T., Flamant, C., Gaetani, M. and Guichard, F.: The past, present and future of African dust, Nature, 531(7595), 493–495, doi:10.1038/nature17149, 2016.

Filonchyk, M. and Peterson, M.: Development, progression, and impact on urban air quality of the dust storm in Asia in March 15–18, 2021, Urban Clim., 41, 101080, doi:10.1016/j.uclim.2021.101080, 2022.

Francis, D., Fonseca, R., Nelli, N., Cuesta, J., Weston, M., Evan, A. and Temimi, M.: The Atmospheric Drivers of the Major Saharan Dust Storm in June 2020, Geophys. Res. Lett., 47(24), doi:10.1029/2020GL090102, 2020.

Francis, D., Nelli, N., Fonseca, R., Weston, M., Flamant, C. and Cherif, C.: The dust load and radiative impact associated with the June 2020 historical Saharan dust storm, Atmos. Environ., 268, 118808, doi:10.1016/j.atmosenv.2021.118808, 2022.

Gelaro, R., McCarty, W., Suárez, M. J., Todling, R., Molod, A., Takacs, L., Randles, C. A., Darmenov, A., Bosilovich, M. G., Reichle, R., Wargan, K., Coy, L., Cullather, R., Draper, C., Akella, S., Buchard, V., Conaty, A., da Silva, A. M., Gu, W., Kim, G.-K., Koster, R., Lucchesi, R., Merkova, D., Nielsen, J. E., Partyka, G., Pawson, S., Putman, W., Rienecker, M., Schubert, S. D., Sienkiewicz, M. and Zhao, B.: The Modern-Era Retrospective Analysis for Research and Applications, Version 2 (MERRA-2), J. Clim., 30(14), 5419–5454, doi:10.1175/JCLI-D-16-0758.1, 2017.

Ginoux, P., Prospero, J. M., Gill, T. E., Hsu, N. C. and Zhao, M.: Global-scale attribution of anthropogenic and natural dust sources and their emission rates based on MODIS Deep Blue aerosol products, Rev. Geophys., 50(3), doi:10.1029/2012RG000388, 2012.

Govarchin-Ghale, Y. A., Tayanc, M. and Unal, A.: Dried bottom of Urmia Lake as a new source of dust in the northwestern Iran: Understanding the impacts on local and regional air quality, Atmos. Environ., 262, 118635,

https://doi.org/10.5194/egusphere-2023-3083
Preprint. Discussion started: 23 February 2024

doi:10.1016/j.atmosenv.2021.118635, 2021.

Gui, K., Yao, W., Che, H., An, L., Zheng, Y., Li, L., Zhao, H., Zhang, L., Zhong, J., Wang, Y. and Zhang, X.: Record-breaking dust loading during two mega dust storm events over northern China in March 2021: aerosol optical and radiative properties and meteorological drivers, Atmos. Chem. Phys., 22(12), 7905–7932, doi:10.5194/acp-22-7905-2022, 2022.

Guiot, J. and Cramer, W.: Climate change: The 2015 Paris Agreement thresholds and Mediterranean basin ecosystems, Science (80-.)., 354(6311), 465–468, doi:10.1126/science.aah5015, 2016.

Kalnay, E., Kanamitsu, M., Kistler, R., Collins, W., Deaven, D., Gandin, L., Iredell, M., Saha, S., White, G., Woollen, J., Zhu, Y., Leetmaa, A., Reynolds, R., Chelliah, M., Ebisuzaki, W., Hig- gins, W., Janowiak, J., Mo, K. C., Ropelewski, C., Wang, J., Jenne, R. and Joseph, D.: The NCEP/NCAR 40-Year Reanalysis Project, B. Am. Meteorol. Soc., 77, 437–471, 1996.

Kaskaoutis, D. G., Rashki, A., Francois, P., Dumka, U. C., Houssos, E. E. and Legrand, M.: Meteorological regimes modulating dust outbreaks in southwest Asia: The role of pressure anomaly and Inter-Tropical Convergence Zone on the 1–3 July 2014 case, Aeolian Res., 18, 83–97, doi:10.1016/j.aeolia.2015.06.006, 2015.

Kaskaoutis, D. G., Houssos, E. E., Rashki, A., Bartzokas, A., Legrand, M., Francois, P. and Kambezidis, H. D.: Modulation of Atmospheric Dynamics and Dust Emissions in Southwest Asia by the Caspian Sea—Hindu Kush Index, pp. 941–947., 2017.

Kaskaoutis, D. G., Rashki, A., Dumka, U. C., Mofidi, A., Kambezidis, H. D., Psiloglou, B. E., Karagiannis, D., Petrinoli, K. and Gavriil, A.: Atmospheric dynamics associated with exceptionally dusty conditions over the eastern Mediterranean and Greece in March 2018, Atmos. Res., 218, 269–284, doi:10.1016/j.atmosres.2018.12.009, 2019.

Katra, I.: Soil Erosion by Wind and Dust Emission in Semi-Arid Soils Due to Agricultural Activities, Agronomy, 10(1), 89, doi:10.3390/agronomy10010089, 2020.

Kok, J. F., Storelvmo, T., Karydis, V. A., Adebiyi, A. A., Mahowald, N. M., Evan, A. T., He, C. and Leung, D. M.: Mineral dust aerosol impacts on global climate and climate change, Nat. Rev. Earth Environ., 4(2), 71–86, doi:10.1038/s43017-022-00379-5, 2023.

Kutuzov, S., Legrand, M., Preunkert, S., Ginot, P., Mikhalenko, V., Shukurov, K., Poliukhov, A. and Toropov, P.: The Elbrus (Caucasus, Russia) ice core record – Part 2: history of desert dust deposition, Atmos. Chem. Phys., 19(22), 14133–14148, doi:10.5194/acp-19-14133-2019, 2019.

Lambert, A., Hallar, A. G., Garcia, M., Strong, C., Andrews, E. and Hand, J. L.: Dust Impacts of Rapid Agricultural Expansion on the Great Plains, Geophys. Res. Lett., 47(20), doi:10.1029/2020GL090347, 2020.

Li, J., Chen, B., de la Campa, A. M. S., Alastuey, A., Querol, X. and de la Rosa, J. D.: 2005–2014 trends of PM10 source

https://doi.org/10.5194/egusphere-2023-3083
Preprint. Discussion started: 23 February 2024

contributions in an industrialized area of southern Spain, Environ. Pollut., 236, 570–579, doi:10.1016/j.envpol.2018.01.101, 2018.

Liu, J., Wu, D., Liu, G., Mao, R., Chen, S., Ji, M., Fu, P., Sun, Y., Pan, X., Jin, H., Zhou, Y. and Wang, X.: Impact of Arctic amplification on declining spring dust events in East Asia, Clim. Dyn., 54(3–4), 1913–1935, doi:10.1007/s00382-019-05094-4, 2020.

Lorentzou, C., Kouvarakis, G., Kozyrakis, G. V, Kampanis, N. A., Trahanatzi, I., Fraidakis, O., Tzanakis, N., Kanakidou, M., Agouridakis, P. and Notas, G.: Extreme desert dust storms and COPD morbidity on the island of Crete, Int. J. Chron. Obstruct. Pulmon. Dis., Volume 14, 1763–1768, doi:10.2147/COPD.S208108, 2019.

Mann, M. E., Rahmstorf, S., Kornhuber, K., Steinman, B. A., Miller, S. K. and Coumou, D.: Influence of Anthropogenic Climate Change on Planetary Wave Resonance and Extreme Weather Events, Sci. Rep., 7(1), 45242, doi:10.1038/srep45242, 2017.

Meinander, O., Kouznetsov, R., Uppstu, A., Sofiev, M., Kaakinen, A., Salminen, J., Rontu, L., Welti, A., Francis, D., Piedehierro, A. A., Heikkilä, P., Heikkinen, E. and Laaksonen, A.: African dust transport and deposition modelling verified through a citizen science campaign in Finland, Sci. Rep., 13(1), 21379, doi:10.1038/s41598-023-46321-7, 2023.

Middleton, N., Kashani, S. S., Attarchi, S., Rahnama, M. and Mosalman, S. T.: Synoptic Causes and Socio-Economic Consequences of a Severe Dust Storm in the Middle East, Atmosphere (Basel)., 12(11), 1435, doi:10.3390/atmos12111435, 2021.

Millán-Martínez, M., Sánchez-Rodas, D., Sánchez de la Campa, A. M. and de la Rosa, J.: Contribution of anthropogenic and natural sources in PM10 during North African dust events in Southern Europe, Environ. Pollut., 290, 118065, doi:10.1016/j.envpol.2021.118065, 2021.

Miri, A. and Middleton, N.: Long-term impacts of dust storms on transport systems in south-eastern Iran, Nat. Hazards, 114(1), 291–312, doi:10.1007/s11069-022-05390-z, 2022.

Mona, L., Amiridis, V., Cuevas, E., Gkikas, A., Trippetta, S., Vandenbussche, S., Benedetti, A., Dagsson-Waldhauserova, P., Formenti, P., Haefele, A., Kazadzis, S., Knippertz, P., Laurent, B., Madonna, F., Nickovic, S., Papagiannopoulos, N., Pappalardo, G., García-Pando, C. P., Popp, T., Rodríguez, S., Sealy, A., Sugimoto, N., Terradellas, E., Vimic, A. V., Weinzierl, B. and Basart, S.: OBSERVING MINERAL DUST IN NORTHERN AFRICA, THE MIDDLE EAST AND EUROPE: CURRENT CAPABILITIES AND CHALLENGES AHEAD FOR THE DEVELOPMENT OF DUST SERVICES, Bull. Am. Meteorol. Soc., doi:10.1175/BAMS-D-23-0005.1, 2023.

Monteiro, A., Basart, S., Kazadzis, S., Votsis, A., Gkikas, A., Vandenbussche, S., Tobias, A., Gama, C., García-Pando, C. P., Terradellas, E., Notas, G., Middleton, N., Kushta, J., Amiridis, V., Lagouvardos, K., Kosmopoulos, P., Kotroni, V., Kanakidou,

https://doi.org/10.5194/egusphere-2023-3083
Preprint. Discussion started: 23 February 2024

M., Mihalopoulos, N., Kalivitis, N., Dagsson-Waldhauserová, P., El-Askary, H., Sievers, K., Giannaros, T., Mona, L., Hirtl, M., Skomorowski, P., Virtanen, T. H., Christoudias, T., Di Mauro, B., Trippetta, S., Kutuzov, S., Meinander, O. and Nickovic, S.: Multi-sectoral impact assessment of an extreme African dust episode in the Eastern Mediterranean in March 2018, Sci. Total Environ., 843, 156861, doi:10.1016/j.scitotenv.2022.156861, 2022.

Mulitza, S., Heslop, D., Pittauerova, D., Fischer, H. W., Meyer, I., Stuut, J.-B., Zabel, M., Mollenhauer, G., Collins, J. A., Kuhnert, H. and Schulz, M.: Increase in African dust flux at the onset of commercial agriculture in the Sahel region, Nature, 466(7303), 226–228, doi:10.1038/nature09213, 2010.

Nishonov, B. E., Kholmatjanov, B. M., Labzovskii, L. D., Rakhmatova, N., Shardakova, L., Abdulakhatov, E. I., Yarashev, D. U., Toderich, K. N., Khujanazarov, T. and Belikov, D. A.: Study of the strongest dust storm occurred in Uzbekistan in November 2021, Sci. Rep., 13(1), 20042, doi:10.1038/s41598-023-42256-1, 2023.

Peshev, Z., Chaikovsky, A., Evgenieva, T., Pescherenkov, V., Vulkova, L., Deleva, A. and Dreischuh, T.: Combined Characterization of Airborne Saharan Dust above Sofia, Bulgaria, during Blocking-Pattern Conditioned Dust Episode in February 2021, Remote Sens., 15(15), 3833, doi:10.3390/rs15153833, 2023.

Pey, J., Querol, X., Alastuey, A., Forastiere, F. and Stafoggia, M.: African dust outbreaks over the Mediterranean Basin during 2001–2011: PM₁₀ concentrations, phenomenology and trends, and its relation with synoptic and mesoscale meteorology, Atmos. Chem. Phys., 13(3), 1395–1410, doi:10.5194/acp-13-1395-2013, 2013.

Pi, H., Huggins, D. R., Abatzoglou, J. T. and Sharratt, B.: Modeling Soil Wind Erosion From Agroecological Classes of the Pacific Northwest in Response to Current Climate, J. Geophys. Res. Atmos., 125(2), doi:10.1029/2019JD031104, 2020.

Preunkert, S., Legrand, M., Kutuzov, S., Ginot, P., Mikhalenko, V. and Friedrich, R.: The Elbrus (Caucasus, Russia) ice core record – Part 1: reconstruction of past anthropogenic sulfur emissions in south-eastern Europe, Atmos. Chem. Phys., 19(22), 14119–14132, doi:10.5194/acp-19-14119-2019, 2019.

Prospero, J. M. ., Ginoux, P., Torres, O., Nicholson, S. E. . and Gill, T. E. .: Environmental characterization of global sources of atmospheric soil dust identified with the Nimbus 7 Total Ozone Mapping Spectrometer (TOMS) absorbing aerosol product, Rev. Geophys., 40(1), 2-1-2–31, doi:10.1029/2000RG000095, 2002.

Pu, B. and Jin, Q.: A Record-Breaking Trans-Atlantic African Dust Plume Associated with Atmospheric Circulation Extremes in June 2020, Bull. Am. Meteorol. Soc., 102(7), E1340–E1356, doi:10.1175/BAMS-D-21-0014.1, 2021.

Qor-El-Aine, A., Béres, A. and Géczi, G.: Case Study of the Saharan Dust Effects on PM10 and PM2.5 Concentrations in Budapest in March 2022, J. Cent. Eur. Green Innov., 10(Suppl 1), 67–78, doi:10.33038/jcegi.3500, 2022.

Querol, X., Alastuey, A., Pandolfi, M., Reche, C., Pérez, N., Minguillón, M. C., Moreno, T., Viana, M., Escudero, M., Orio, A., Pallarés, M. and Reina, F.: 2001–2012 trends on air quality in Spain, Sci. Total Environ., 490, 957–969,

doi:10.1016/j.scitotenv.2014.05.074, 2014.

Ridley, D. A., Heald, C. L. and Prospero, J. M.: What controls the recent changes in African mineral dust aerosol across the Atlantic?, Atmos. Chem. Phys., 14(11), 5735–5747, doi:10.5194/acp-14-5735-2014, 2014.

Rodriguez-Caballero, E., Stanelle, T., Egerer, S., Cheng, Y., Su, H., Canton, Y., Belnap, J., Andreae, M. O., Tegen, I., Reick, C. H., Pöschl, U. and Weber, B.: Global cycling and climate effects of aeolian dust controlled by biological soil crusts, Nat. Geosci., 15(6), 458–463, doi:10.1038/s41561-022-00942-1, 2022.

Rodríguez, S. and López-Darias, J.: Dust and tropical PMx aerosols in Cape Verde: Sources, vertical distributions and stratified transport from North Africa, Atmos. Res., 263, 105793, doi:10.1016/j.atmosres.2021.105793, 2021.

Rodríguez, S., Querol, X., Alastuey, A., Kallos, G. and Kakaliagou, O.: Saharan dust contributions to PM10 and TSP levels in Southern and Eastern Spain, Atmos. Environ., 35(14), 2433–2447, doi:10.1016/S1352-2310(00)00496-9, 2001.

Rodríguez, S., Alastuey, A., Alonso-Pérez, S., Querol, X., Cuevas, E., Abreu-Afonso, J., Viana, M., Pérez, N., Pandolfi, M. and de la Rosa, J.: Transport of desert dust mixed with North African industrial pollutants in the subtropical Saharan Air Layer, Atmos. Chem. Phys., 11(13), 6663–6685, doi:10.5194/acp-11-6663-2011, 2011.

Rodríguez, S., Alastuey, A. and Querol, X.: A review of methods for long term in situ characterization of aerosol dust, Aeolian Res., 6, 55–74, doi:10.1016/j.aeolia.2012.07.004, 2012.

Rodríguez, S., Cuevas, E., Prospero, J. M., Alastuey, A., Querol, X., López-Solano, J., García, M. I. and Alonso-Pérez, S.: Modulation of Saharan dust export by the North African dipole, Atmos. Chem. Phys., 15(13), 7471–7486, doi:10.5194/acp-15-7471-2015, 2015.

Rodríguez, S., Riera, R., Fonteneau, A., Alonso-Pérez, S. and López-Darias, J.: African desert dust influences migrations and fisheries of the Atlantic skipjack-tuna, Atmos. Environ., 312, 120022, doi:10.1016/j.atmosenv.2023.120022, 2023.

Seidel, D. J., Fu, Q., Randel, W. J. and Reichler, T. J.: Widening of the tropical belt in a changing climate, Nat. Geosci., 1(1), 21–24, doi:10.1038/ngeo.2007.38, 2008.

Solomos, S., Kalivitis, N., Mihalopoulos, N., Amiridis, V., Kouvarakis, G., Gkikas, A., Binietoglou, I., Tsekeri, A., Kazadzis, S., Kottas, M., Pradhan, Y., Proestakis, E., Nastos, P. and Marenco, F.: From Tropospheric Folding to Khamsin and Foehn Winds: How Atmospheric Dynamics Advanced a Record-Breaking Dust Episode in Crete, Atmosphere (Basel)., 9(7), 240, doi:10.3390/atmos9070240, 2018.

Tong, D. Q., Gill, T. E., Sprigg, W. A., Van Pelt, R. S., Baklanov, A. A., Barker, B. M., Bell, J. E., Castillo, J., Gassó, S., Gaston, C. J., Griffin, D. W., Huneeus, N., Kahn, R. A., Kuciauskas, A. P., Ladino, L. A., Li, J., Mayol-Bracero, O. L., McCotter, O. Z., Méndez-Lázaro, P. A., Mudu, P., Nickovic, S., Oyarzun, D., Prospero, J., Raga, G. B., Raysoni, A. U., Ren,

https://doi.org/10.5194/egusphere-2023-3083
Preprint. Discussion started: 23 February 2024

L., Sarafoglou, N., Sealy, A., Sun, Z. and Vimic, A. V.: Health and Safety Effects of Airborne Soil Dust in the Americas and Beyond, Rev. Geophys., 61(2), doi:10.1029/2021RG000763, 2023.

Viana, M., Querol, X., Alastuey, A., Cuevas, E. and Rodríguez, S.: Influence of African dust on the levels of atmospheric particulates in the Canary Islands air quality network, Atmos. Environ., 36(38), 5861–5875, doi:10.1016/S1352-2310(02)00463-6, 2002.

Vukovic, A., Cvetkovic, B., Giannaros, T., Shahbazi, R., Sehat Kashani, S., Prieto, J., Kotroni, V., Lagouvardos, K., Pejanovic, G., Petkovic, S., Nickovic, S., Vujadinovic, M., Basart, S., Darvishi, A. and Terradellas, E.: Numerical Simulation of Tehran Dust Storm on 2 June 2014: A Case Study of Agricultural Abandoned Lands as Emission Sources, Atmosphere (Basel)., 12(8), 1054, doi:10.3390/atmos12081054, 2021.

Xi, X., Steinfeld, D., Cavallo, S., Wang, J., Chen, J., Zulpykharov, K. and Henebry, G. M.: What caused the unseasonal extreme dust storm in Uzbekistan during November 2021?, Environ. Res. Lett., doi:10.1088/1748-9326/ad02af, 2023.

Yang, H., Lohmann, G., Lu, J., Gowan, E. J., Shi, X., Liu, J. and Wang, Q.: Tropical Expansion Driven by Poleward Advancing Midlatitude Meridional Temperature Gradients, J. Geophys. Res. Atmos., 125(16), doi:10.1029/2020JD033158, 2020.

Yang, H., Lohmann, G., Shi, X. and Müller, J.: Evaluating the Mechanism of Tropical Expansion Using Idealized Numerical Experiments, Ocean. Res., 2, doi:10.34133/olar.0004, 2023.

Yu, H., Chin, M., Yuan, T., Bian, H., Remer, L. A., Prospero, J. M., Omar, A., Winker, D., Yang, Y., Zhang, Y., Zhang, Z. and Zhao, C.: The fertilizing role of African dust in the Amazon rainforest: A first multiyear assessment based on data from Cloud-Aerosol Lidar and Infrared Pathfinder Satellite Observations, Geophys. Res. Lett., 42(6), 1984–1991, doi:10.1002/2015GL063040, 2015.

Yu, H., Tan, Q., Zhou, L., Zhou, Y., Bian, H., Chin, M., Ryder, C. L., Levy, R. C., Pradhan, Y., Shi, Y., Song, Q., Zhang, Z., Colarco, P. R., Kim, D., Remer, L. A., Yuan, T., Mayol-Bracero, O. and Holben, B. N.: Observation and modeling of the historic “Godzilla” African dust intrusion into the Caribbean Basin and the southern US in June 2020, Atmos. Chem. Phys., 21(16), 12359–12383, doi:10.5194/acp-21-12359-2021, 2021.

Yu, Y. and Ginoux, P.: Enhanced dust emission following large wildfires due to vegetation disturbance, Nat. Geosci., 15(11), 878–884, doi:10.1038/s41561-022-01046-6, 2022.

Zafra-Pérez, A., Boente, C., García-Díaz, M., Gómez-Galán, J. A., de la Campa, A. S. and de la Rosa, J. D.: Aerial monitoring of atmospheric particulate matter produced by open-pit mining using low-cost airborne sensors, Sci. Total Environ., 904, 166743, doi:10.1016/j.scitotenv.2023.166743, 2023.

Zhang, T., Zheng, M., Sun, X., Chen, H., Wang, Y., Fan, X., Pan, Y., Quan, J., Liu, J., Wang, Y., Lyu, D., Chen, S., Zhu, T. and Chai, F.: Environmental impacts of three Asian dust events in the northern China and the northwestern Pacific in spring

https://doi.org/10.5194/egusphere-2023-3083
Preprint. Discussion started: 23 February 2024

2021, Sci. Total Environ., 859, 160230, doi:10.1016/j.scitotenv.2022.160230, 2023.